BIOCHEMISTRY
including biophysical chemistry & molecular biology

Article

pubs.acs.org/biochemistry

Efficacy as an Intrinsic Property of the M_2 Muscarinic Receptor in Its Tetrameric State

Dar'ya S. Redka, Heiko Heerklotz, and James W. Wells*

Department of Pharmaceutical Sciences, Leslie Dan Faculty of Pharmacy, University of Toronto, Toronto, Ontario, Canada M5S 3M2

Supporting Information

ABSTRACT: Muscarinic and other G protein-coupled receptors exhibit an agonist-specific heterogeneity that tracks efficacy and commonly is attributed to an effect of the G protein on an otherwise homogeneous population of sites. To examine this notion, M_2 muscarinic receptors were purified from *Sf*9 cells as monomers devoid of G protein and reconstituted as tetramers in phospholipid vesicles. In assays with *N*-[^{3}H]methylscopolamine, seven agonists revealed a dispersion of affinities indicative of two or more classes of sites. Unlabeled *N*-methylscopolamine and the antagonist quinuclidinylbenzilate recognized one class of sites; atropine recognized two classes with a preference that was the opposite of that of agonists, as indicated by the effects of *N*-ethylmaleimide. The data were inconsistent with an explicit model of constitutive asymmetry within a tetramer, and the fit improved markedly upon the introduction of cooperative interactions ($P < 0.00001$). Purified monomers appeared to be homogeneous or nearly so to all ligands except the partial agonists pilocarpine and McN-A-343, where heterogeneity emerged from intramolecular cooperativity between the orthosteric site and an allosteric site. The breadth of each dispersion was quantified empirically as the area between the fitted curve for two classes of sites and the theoretical curve for a single class of lower affinity, which approximates the expected effect of GTP if a G protein were present. The areas measured for 10 ligands at reconstituted tetramers correlated with similar measures of heterogeneity and with intrinsic activities reported previously for binding and response in natural membranes ($P \leq 0.00002$). The data suggest that the GTP-sensitive heterogeneity typically revealed by agonists at M_2 receptors is intrinsic to the receptor in its tetrameric state. It exists independently of the G protein, and it appears to arise at least in part from cooperativity between linked orthosteric sites.

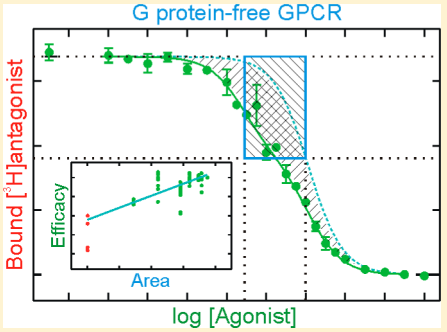

G protein-coupled receptors display an intriguing dispersion of affinities in the binding of agonists, which distinguish two or more classes of sites. The heterogeneity is sensitive to guanylyl nucleotides, which steepen the binding profile and move it rightward in an apparent interconversion of sites from higher to lower affinity. Both the breadth of the dispersion and the magnitude of the shift are a measure of efficacy,[1−3] and the phenomenon therefore offers a window into the mechanism of signaling at the level of the receptor. Such effects have been described extensively for GPCRs of Family 1, including the muscarinic,[1,3,4] dopamine,[5] serotonin,[6] α-adrenergic,[7] and β-adrenergic receptors.[2,8]

A widely cited explanation for such behavior is the ternary complex model,[9] in which the heterogeneity is attributed to a ligand-regulated equilibrium between receptors (R) and G proteins on the one hand and a transient RG complex on the other (i.e., R + G ⇌ RG). Agonists (A) bind with higher affinity to the complex than to the free receptor and therefore promote coupling; antagonists[a] are indifferent or favor the uncoupled state. Guanylyl nucleotides such as GDP, GTP, and GMP-PNP promote uncoupling,[10] which in the case of GTP and GMP-PNP is accompanied by fragmentation of the G protein into the α-subunit and $\beta\gamma$ heterodimer.[11−13] GDP formed by the hydrolysis of GTP permits reassembly of the holo-G protein and its reassociation with the receptor in the presence of an agonist.[14]

The heterogeneity observed in assays conducted at thermodynamic equilibrium arises from the coexistence of uncoupled and G protein-coupled receptors, although the nature of the effect depends upon the relative numbers of receptors and G proteins; the nucleotide-induced shift arises from an imbalance in which the nucleotide outbids the agonist in its effect on the equilibrium between R and RG.

In accord with the notion of a transient complex favored or disfavored by ligands, the association of GPCRs with G proteins can be enhanced by agonists[15−17] and inhibited or prevented by antagonists.[16,18] Also, the position of the supposed equilibrium in the absence of ligands can vary from fully uncoupled and inactive[15,17] to partially coupled and therefore constitutively active,[19,20] depending upon factors such as the environment[19] or mutations in the receptor.[21−23] Perhaps most persuasively, the level of constitutive activity and the potencies of agonists were increased by overexpression of $G\alpha_q$ in the case of M_1, M_3, and M_5 muscarinic receptors in NIH-3T3 cells.[24]

Schemes based on a transient complex have proven to be difficult to confirm directly, in part because of the ambiguity of

Received: March 25, 2013
Revised: September 15, 2013
Published: September 19, 2013

the data. For example, ligand-dependent effects identified by co-immunoprecipitation (e.g., ref 16) may reflect the survival of a preexisting complex during solubilization rather than the state of the system in the membrane. Similarly, a ligand-induced decrease in the level of resonance energy transfer may reflect a conformational change rather than a process in which one G protein dissociates to join a pool from which it is replaced by another (e.g., refs 25 and 26). Moreover, the possibility that the complex is less transient than required by such models is suggested by its stability during purification,[27,28] its properties in reconstituted systems,[18] and its formation early in the biosynthetic pathway.[29]

Questions with respect to a transient complex also arise from the ternary complex model itself. When applied in a mechanistically consistent manner, variants of the model have failed to describe the binding of agonists and guanylyl nucleotides to M_2 receptors and associated G proteins in myocardial membranes.[30,31] In its original application to β-adrenergic receptors in membranes from frog erythrocytes, agreement with the data required that the ratio of total G protein to total receptor vary from agonist to agonist and decrease in the presence of GMP-PNP.[9] Similarly, nucleotide-dependent changes in the number of G proteins were required for the model to account for the effect of GMP-PNP on the binding of carbachol to cardiac muscarinic receptors.[32] Such adjustments violate the assumption that ligands act by virtue of their relative affinities for the uncoupled and coupled states. Agreement also has required that receptors outnumber G proteins or occur in equimolar amounts.[3,30,31] Because G proteins can outnumber receptors by 20−240-fold overall,[7,33] such a condition implies that most G proteins reside in a receptor-free compartment.[7]

A common feature of the ternary complex model and similar proposals is the idea that heterogeneity is induced by the G protein in an otherwise homogeneous population of receptors. That explanation is at variance with reports of heterogeneity in the binding of agonists to purified muscarinic receptors,[27,34−36] which suggest rather that heterogeneity is intrinsic to the receptor, perhaps emerging as a consequence of oligomerization.

Many GPCRs are known to form oligomers,[37,38] including muscarinic receptors[39,40] and in particular the M_2 muscarinic receptor.[27,41,42] G proteins also are known to form oligomers,[28,43,44] and a stable heteromeric complex comprising multiple equivalents of the M_2 muscarinic receptor and G proteins has been affinity-purified from porcine atria.[27,28] Such a hetero-oligomer is consistent with a reciprocal arrangement that emerges from the binding of agonists and guanylyl nucleotides: that is, the effect of guanylyl nucleotides on the binding of agonists to the receptor is mirrored by the effect of agonists on the binding of GDP to receptor-linked G proteins.[27,45−47] Muscarinic and other GPCRs also are known to exist in multiple interconverting states.[9,22,48] Taken together, these observations have led to a proposal in which a heteromer of receptors and G proteins interconverts spontaneously between two or more states differing in their degree of cooperativity and perhaps asymmetry in the binding of agonists and guanylyl nucleotides (Scheme 3 of ref 49).

Previous studies of the purified muscarinic receptor did not address its state of aggregation, nor did they consider whether the observed heterogeneity was the same as that observed in natural membranes. In some cases, the absence of copurifying G proteins was not confirmed by direct measurement. We therefore have compared two forms of the M_2 muscarinic receptor purified from *Sf*9 cells and devoid of G proteins: monomers in a micellar dispersion and tetramers reconstituted in phospholipid vesicles. The latter were prepared according to a procedure modified from that described previously,[50] including the substitution of POPC and POPS for lipids extracted from bovine brain and egg yolk. Each preparation was examined for the binding of three muscarinic antagonists (quinuclidinylbenzilate, *N*-methylscopolamine, and atropine) and seven agonists (carbachol, arecoline, bethanechol, oxotremorine-M, oxotremorine, pilocarpine, and McN-A-343). The results indicate that the reconstituted tetramers exhibit a heterogeneity that is similar in kind to that observed with M_2 muscarinic receptors in natural membranes.

MATERIALS AND METHODS

Ligands, Antibodies, and Other Materials. *N*-[^{3}H]-Methylscopolamine was purchased from PerkinElmer Life and Analytical Sciences (lot 3615097, 70 Ci/mmol; lot 3615935, 82 Ci/mmol). (−)-[^{3}H]Quinuclidinylbenzilate was from Amersham Biosciences (lot B52, 48 Ci/mmol). Unlabeled *N*-methylscopolamine hydrobromide, (*R*)-(−)-quinuclidinylbenzilate, atropine sulfate, aminobenztropine, oxotremorine-M, carbamoylcholine chloride (carbachol), carbamyl-β-methylcholine chloride (bethanechol), arecoline hydrobromide, pilocarpine hydrochloride, and guanosine 5′-[β,γ-imido]triphosphate trisodium salt hydrate (GMP-PNP) were purchased from Sigma-Aldrich. Oxotremorine sesquifumarate and McN-A-343 were from Tocris Bioscience.

Suppliers of other chemicals were as follows: BDH, Inc. (magnesium chloride and sodium chloride), Bioshop Canada (dithiothreitol), Caledon Laboratories Ltd. (glycerol), EMD Chemicals, Inc. (methanol), EM Science (sodium dodecyl sulfate and potassium chloride), Pierce Biotechnology, Inc. (BS^3), Roche Diagnostics (HEPES), and Sigma-Aldrich (EDTA, *N*-ethylmaleimide, glycine, magnesium sulfate, PMSF, Trizma base, and Tween 20).

Holo-G proteins were purchased from Calbiochem as a mixture of functional heterotrimers (i.e., $\alpha_o\beta\gamma$ and $\alpha_{i1-3}\beta\gamma$) purified from bovine brain and supplied in solution [50 mM HEPES, 1 mM DTT, 1 mM EDTA, and 0.1% Lubrol (pH 7.6)].

Ex-Cell 420 insect medium was purchased from JRH Biosciences, Inc. Fetal bovine serum, Fungizone, and gentamycin were from Invitrogen. Complete Protease Inhibitor Cocktail tablets were from Roche.

Digitonin used for solubilization and purification of the receptor was purchased from Wako Bioproducts at ∼100% purity. Digitonin used for buffers to pre-equilibrate and elute Sephadex G-50 columns in binding assays was purchased initially from Calbiochem (high purity) and subsequently from Wako. Sodium cholate hydrate and cholesterol were purchased from Sigma-Aldrich. The synthetic phospholipids POPC (16:0−18:1 PC) and POPS (16:0−18:1 PS) were from Avanti Polar Lipids.

Sephadex G-50 (fine) and Fast-Flow DEAE-Sepharose were purchased from GE Healthcare. Polypropylene columns used in the binding assays were purchased from Kontes (Disposaflex, 0.8 cm × 6.5 cm). Econo-Pacs and Econo-Columns were from Bio-Rad Laboratories, and the receptor was concentrated using Centricon and Centriprep concentrators (Amicon) purchased from Millipore. The protein concentration was estimated by means of bicinchoninic acid using the BCA Protein Assay Kit and bovine serum albumin, taken as the standard, purchased from Pierce.

The anti-HA antibody (mouse) conjugated to horseradish peroxidase was purchased from Roche Diagnostics. The agarose-conjugated anti-FLAG antibody (mouse) used for immunopre-

cipitation was from Sigma-Aldrich. The anti-M_2 muscarinic acetylcholine receptor monoclonal antibody (mouse) was purchased from Thermo Scientific.

Muscarinic Receptor. All experiments were performed on the purified human M_2 muscarinic receptor bearing the hemagglutinin (HA) (YPYDVPDYA) or FLAG (DYKDDDDA) epitope at the amino terminus and a hexahistidyl tag at the carboxyl terminus. *Sf*9 cells were cultured at 27 °C in Ex-Cell 420 insect medium containing 2% fetal bovine serum, 1% Fungizone, and 0.01% gentamycin. Cells growing at a density of 2×10^6 cells/mL were co-infected with the two baculoviruses at a total multiplicity of infection of 5 and harvested 48 h later. The membranes were solubilized in digitonin and cholate (0.86% digitonin and 0.17% cholate), and the receptor was purified via successive passage on DEAE-Sepharose, ABT-Sepharose, and hydroxyapatite. The resulting preparation of receptor in buffer A (20 mM KH_2PO_4 adjusted to pH 7.40 with KOH, 20 mM NaCl, 1 mM EDTA, and 0.1 mM PMSF) containing digitonin (0.1%) and cholate (0.02%) was concentrated 3−5-fold such that the final receptor concentration was 100 nM. The concentrated preparation was divided into aliquots (30 μL) that were stored at −75 °C. Further details regarding growth of the cells and purification of the receptor have been described previously.[27,50,51]

Reconstitution in Phospholipid Vesicles. In an earlier study, tetramers of the M_2 muscarinic receptor were reconstituted in vesicles composed of phospholipid extracted from bovine brain and egg yolk.[50] Subsequent work has shown that different batches of lipid can result in mixtures of monomers, dimers, and tetramers under some conditions. Such variability has been avoided by using vesicles prepared from the synthetic lipids POPC and POPS, in which the receptors assemble consistently and almost wholly as tetramers.

POPC (1 mg), POPS (1 mg), and cholesterol (0.06 mg) were dissolved in chloroform and dried uniformly under argon to a thin film.[35,50] The lipids then were hydrated for 1 h at 40 °C in 1 mL of buffer B (20 mM HEPES, 160 mM NaCl, 0.8 mM EDTA, adjusted to pH 8.0 with KOH), followed by three cycles of freezing in liquid nitrogen and thawing. Vesicles were prepared by extrusion through a polycarbonate membrane with 50 nm pores (Nuclepore Track-Etch Membrane, Whatman) mounted on an Avanti Mini-Extruder.

The purified M_2 receptor (3 pmol in 30 μL) was mixed with carbachol (10 mM in 20 μL of buffer B) and kept for 15 min at 4 °C. The sample then was mixed with preformed vesicles (150 μL) and applied to a column of Sephadex G-50 (0.8 cm × 5.0 cm) pre-equilibrated with buffer B.[50] The column was washed with 600 μL of buffer B, and receptor-containing vesicles were eluted with a further 500 μL of the same buffer. The recovery of the receptor and lipid after reconstitution was ∼33% in each case, and the mean ratio of receptors to vesicles was 0.3−0.6 (Supporting Information). To resolubilize the reconstituted receptor when required, the vesicular preparation was supplemented with digitonin (final concentration of 0.86%) and incubated for 2 h at 4 °C.

To reconstitute the receptor together with holo-G proteins, buffer B was supplemented with DTT (1 mM) and $MgCl_2$ (6 mM). An aliquot of G proteins was added to the receptor following incubation of the latter with carbachol for 10 min at 4 °C. The mixture was incubated for an additional 5 min at 4 °C and then was incorporated with the lipids as described above. G proteins were added in a ratio of 10 α-subunits per receptor.

The vesicular size was determined by dynamic light scattering using a Zetasizer Nano ZS analyzer (Malvern Instruments Ltd.) equipped with a He−Ne laser (633 nm) and operating at a scattering angle of 173°. Estimates of the average hydrodynamic size (*Z*-average) and the polydispersity index from each of three or more recordings of the same preparation were averaged to obtain the means, which in turn were averaged to obtain the means over different preparations.

Cross-Linking. An aliquot of the receptor was supplemented with BS^3 in deionized water (20 mM) to yield a final reagent concentration of 2 mM. The mixture was incubated for 30 min at room temperature, and the reaction was terminated by the addition of Tris-HCl (1 M, pH 8.00) to a final concentration of 20 mM. After further incubation for 15 min at room temperature, the sample was placed on ice pending examination by electrophoresis as described below. Samples lacking BS^3 but treated in a parallel and otherwise identical manner were prepared as controls.

Treatment with *N*-Ethylmaleimide. Aliquots of the purified or reconstituted receptor were mixed with a freshly prepared solution of *N*-ethylmaleimide (100 mM) in buffer A or B, respectively, to yield a final reagent concentration of 10 mM. The reaction was conducted on ice for 2 h, and the treated receptor was examined in binding assays. Controls lacking *N*-ethylmaleimide were prepared and assayed in an identical manner. Further details regarding the treatment with *N*-ethylmaleimide have been described previously.[48]

Immunoprecipitation, Electrophoresis, Western Blotting, and Silver Staining. To test for co-immunoprecipitation, aliquots of the tagged receptor (400 μL) were mixed with a 50% slurry of the agarose-conjugated anti-FLAG antibody (20 μL) and shaken overnight at 4 °C. The immunoadsorbed receptor was collected by centrifugation for 5 min at 4 °C and 1000*g*, and the precipitated beads were washed four times by resuspension in 1 mL of buffer C (9.1 mM Na_2HPO_4, 1.7 mM NaH_2PO_4, 150 mM NaCl, adjusted to pH 7.40 with NaOH) and subsequent centrifugation. Further details have been described previously.[50,51]

Samples for electrophoresis were heated at 65 °C for 5 min prior to being loaded on precast polyacrylamide gels from Bio-Rad (Ready Gel Tris-HCl, 10%). It has been shown previously that these conditions do not induce aggregation of the M_2 muscarinic receptor from *Sf*9 cells.[51] Resolved proteins were transferred onto nitrocellulose membranes (Bio-Rad, 0.45 μm) in a Mini Trans-Blot Transfer Cell (Bio-Rad). The membranes then were treated with the primary antibody or the horseradish peroxidase-conjugated antibody for 2 h, both at a dilution of 1:1000. Treatment with the secondary antibody was conducted for 1 h at a dilution of 1:3000. Proteins were visualized by chemiluminescence using reagents and film purchased from GE Healthcare (ECL, Hyperfilm MP). The images were digitized at a resolution of 300 dots per inch, and the intensities of the bands were estimated from the densitometric trace using ImageJ.[52]

Silver staining was conducted using the ProteoSilver kit from Sigma-Aldrich. Stained gels were photographed in a Trans-illuminator Gel Documentation System (UVP, model M-20) equipped with an 8-bit camera. The density was quantified using ImageJ,[52] and the areas of the peaks were estimated by Gaussian deconvolution using PeakFit (Systat) as described previously.[50]

Binding Assays. The radioligand and any unlabeled ligand were dissolved in buffer D (25 mM KH_2PO_4, 4 mM HEPES adjusted to pH 8.00 with KOH, 230 mM NaCl, 0.8 mM EDTA, 10 mM $MgCl_2$, 0.1 mM PMSF, adjusted to pH 7.40 with NaOH).

For assays of the purified receptor in solution, buffer D was supplemented with 0.1% digitonin and 0.02% cholate. An aliquot of the ligand-containing solution (49 μL) was added to the solubilized or reconstituted receptor (4 μL) in a polypropylene microcentrifuge tube, and the reaction mixture was incubated at 30 °C for 2 h in the case of [^{3}H]quinuclidinylbenzilate and for 45 min in the case of *N*-[^{3}H]methylscopolamine. The bound radioligand then was separated by applying an aliquot (50 μL) to a column of Sephadex G-50 fine (0.8 cm × 6.5 cm) pre-equilibrated with buffer E (20 mM HEPES, 20 mM NaCl, 5 mM $MgSO_4$, 1 mM EDTA, adjusted to pH 7.40 with NaOH) supplemented with 0.017% digitonin. The assays were performed in triplicate. Nonspecific binding was estimated in the presence of 1 mM unlabeled *N*-methylscopolamine.

Analysis of Data. All data were analyzed with total binding taken as the dependent variable (B_{obsd}) and the total concentrations of all ligands taken as the independent variables. The free concentration of a ligand was calculated numerically from the total concentration as required. The values listed for total receptor ($[R]_t$), maximal specific binding (B_{max}), and the concentrations of ligands are the concentrations in the binding assays.

Data acquired at graded concentrations of [^{3}H]-quinuclidinylbenzilate or *N*-[^{3}H]methylscopolamine were analyzed empirically according to the Hill equation, formulated as shown in eq 1,

$$B_{obsd} = B_{max}\frac{([P]_t - B_{sp})^{n_H}}{EC_{50}{}^{n_H} + ([P]_t - B_{sp})^{n_H}} + NS([P]_t - B_{sp}) \quad (1)$$

where B_{max} represents the maximal specific binding of the radioligand (P) and B_{sp} represents the specific binding at total concentration $[P]_t$. The parameter EC_{50} represents the concentration of unbound radioligand that corresponds to half-maximal specific binding, and n_H is the Hill coefficient. The parameter NS represents the fraction of unbound radioligand that appears as nonspecific binding, which was found to increase linearly with the concentration of unbound [^{3}H]-quinuclidinylbenzilate or *N*-[^{3}H]methylscopolamine.

For data acquired at a single concentration of *N*-[^{3}H]-methylscopolamine and graded concentrations of an unlabeled ligand, the Hill equation was formulated as shown in eq 2.

$$B_{obsd} = (B_{[A]=0} - B_{[A]\to\infty})\frac{IC_{50}{}^{n_H}}{IC_{50}{}^{n_H} + [A]_t{}^{n_H}} + B_{[A]\to\infty} \quad (2)$$

The variable $[A]_t$ is the total concentration of unlabeled ligand, and IC_{50} is the value of $[A]_t$ that corresponds to half-maximal inhibition of specific binding of the radioligand. The parameters $B_{[A]=0}$ and $B_{[A]\to\infty}$ represent the asymptotic levels of binding when $[A]_t = 0$ and as $[A]_t \to \infty$, respectively.

Such data also were analyzed empirically as a sum of hyperbolic terms, formulated as shown in eq 3.

$$B_{obsd} = (B_{[A]=0} - B_{[A]\to\infty})\sum_{j=1}^{n}\frac{F_j IC_{50(j)}}{IC_{50(j)} + [A]_t} + B_{[A]\to\infty} \quad (3)$$

The parameter $IC_{50(j)}$ represents the total concentration of unlabeled ligand that corresponds to half-maximal inhibition at fraction F_j of labeled sites ($\Sigma_{j=1}^{n}F_j = 1$), and other parameters are as defined above. When *n* equals 2, the parameters F_1 and F_2 are designated F_H and F_L, respectively; similarly, $IC_{50(1)}$ and $IC_{50(2)}$ are designated $IC_{50(H)}$ and $IC_{50(L)}$, respectively.

The degree of heterogeneity revealed in a semilogarithmic binding profile was quantified in terms of eq 3 as the area between the fitted curve obtained with two classes of sites ($n = 2$) and the theoretical curve corresponding to a single class ($n = 1$) of equal amplitude and the weaker of the two affinities defined by the data (Figure 1). As shown in the Supporting Information,

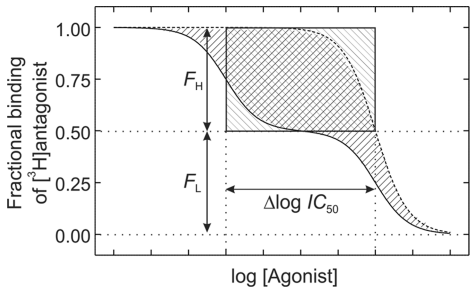

Figure 1. Quantification of heterogeneity and the potential effect of GTP. Data were simulated according to eq 3 with two terms [$IC_{50(H)} = IC_{50(L)} \times 10^{-4}$, and $F_H = 0.5$] (—) or with one term (---) such that the single value of IC_{50} equals the value of $IC_{50(L)}$ when $n = 2$. The area between the two curves (forward hatches) equals that of the rectangle defined by the relative potency of the ligand for the two classes of sites {i.e., $\Delta\log IC_{50} = \log[IC_{50(L)}/IC_{50(H)}]$} and the fractional amplitude corresponding to $IC_{50(H)}$ (i.e., F_H) (backward hatches). Further details are described in the Supporting Information.

that area is equal to the area of the rectangle defined by the amplitude of the high-affinity component of the fitted curve and the corresponding difference in the affinity of the ligand for the two sites (i.e., $F_H \times \Delta\log IC_{50}$). In the case of the M_2 muscarinic receptor or another GPCR, it is a measure of the change effected by a guanylyl nucleotide in causing the apparent interconversion of sites from higher to lower affinity for agonists.

Mechanistic analyses were performed in terms of Schemes 1–3, in which heterogeneity arises from a static mixture of

Scheme 1

$$PR_j \underset{[P]/K_{Pj}}{\rightleftharpoons} R_j \overset{[A]/K_{Aj}}{\rightleftharpoons} AR_j$$

Scheme 2

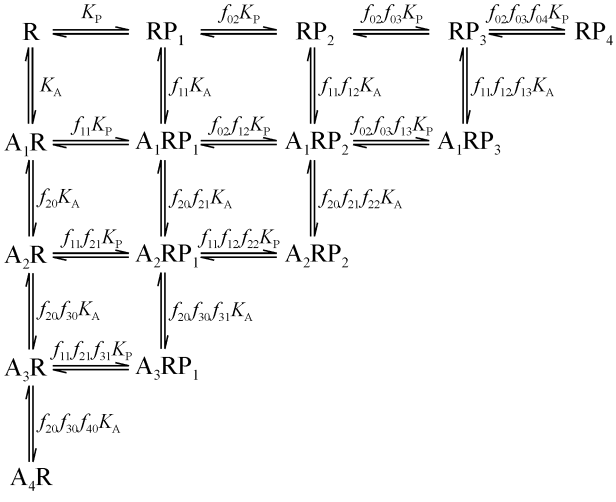

Scheme 3

dx.doi.org/10.1021/bi4003869 | *Biochemistry* 2013, 52, 7405–7427

Scheme 3

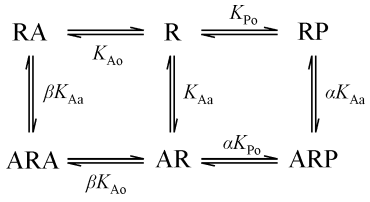

independent and distinct sites (Scheme 1), cooperativity among four interacting but otherwise identical sites (Scheme 2), and cooperativity between two pharmacologically distinct sites (Scheme 3). Estimates of total binding were fit by the equation $B_{obsd} = B_{sp} + NS([P]_t - B_{sp})$, in which the variables and parameters are as described above for eq 1. The value of B_{sp} was computed according to each scheme as described below.

Scheme 1 depicts an intrinsically heterogeneous system in which the radioligand (P) and an unlabeled ligand (A) compete for distinct and mutually independent sites (R_j, where $j = 1, 2, ..., n$). Sites of type j bind P and A with equilibrium dissociation constants K_{Pj} and K_{Aj}, respectively, and constitute the fraction F_j of all sites (i.e., $F_j = [R_j]_t/[R]_t$, where $[R_j]_t = [R_j] + [AR_j] + [PR_j]$, and $[R]_t = \sum_{j=1}^{n}[R_j]_t$). In the special case of four independent sites within a tetramer, F_j was set equal to 0.25 for each j. The total specific binding of the probe was calculated according to eq 4, in which the required values of $[PR_j]$ were calculated from the total concentrations of the receptor (i.e., $[R_j]_t$) and the free concentrations of A and P; the latter were computed numerically from the total concentrations as described previously.[53]

$$B_{sp} = \sum_{j=1}^{n} [PR_j] \quad (4)$$

Scheme 2 depicts a tetravalent receptor that can bind up to 4 equiv of either P or A. The receptor presumably is a tetramer, and it is assumed that its oligomeric status remains unchanged under the conditions of the binding assays. There can be no exchange of subunits within the system, but the model can accommodate processes in which dissociated monomers regroup without exchanging partners.

The vacant receptor exists in a single state designated R. Asymmetry cannot be detected with the present data, and all of the sites are assumed to bind P or A with microscopic dissociation constant K_P or K_A, respectively [e.g., $K_P = ([P][R])/[PR]$]. Similarly, the microscopic dissociation constant was taken to be the same for all vacant sites on a partially liganded receptor [e.g., $([P][POOA])/[PPOA] = ([P][POOA])/[POPA]$, where O represents a vacant site on a tetravalent receptor]. Parameters f_{i0} and f_{0j} represent the cooperativity factors for the binding of the ith equivalent of A ($i \geq 2$) and the jth equivalent of P ($j \geq 2$) to form A_iR and RP_j, respectively [e.g., $([RP_{j-1}][P])/[RP_j] = \Pi_{k=2}^{j} f_{0k}K_P$]. The parameters f_{ij} represent cooperativity factors in the formation of mixed complexes (i.e., A_iRP_j). Either form of cooperativity may be positive ($f < 1$) or negative ($f > 1$). The value of f_{00}, f_{10}, and f_{01} is defined as 1 in each case.

The total specific binding of the probe in Scheme 2 was calculated according to eq 5. The required values of $[A_iRP_j]$ were calculated from $[R]_t$ and the free concentrations of A and P; the latter were computed numerically from $[A]_t$ and $[P]_t$ as described previously.[53]

$$B_{sp} = \sum_{j=1}^{4}\sum_{i=0}^{4-j} j\binom{4}{j}\binom{4-j}{i}[A_iRP_j] \quad (5)$$

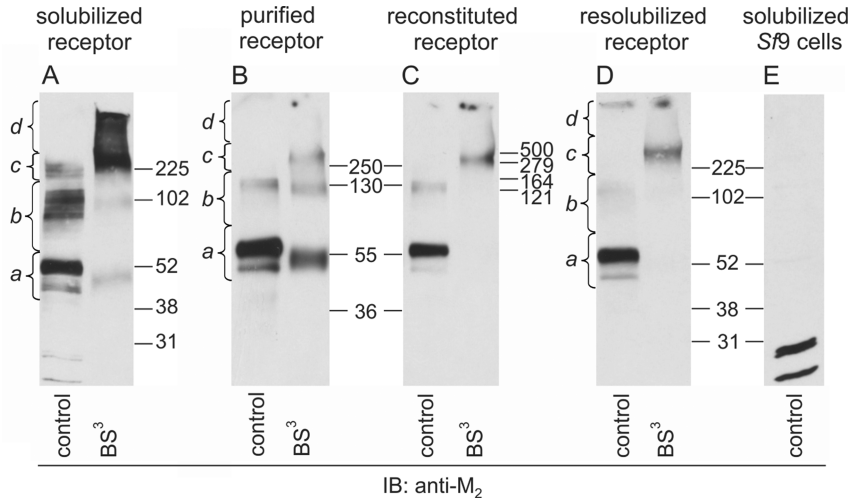

Figure 2. Detection of monomers and oligomers in preparations of the M_2 muscarinic receptor. Gels were loaded with samples of unprocessed extract (A), purified receptor (B), purified receptor reconstituted into phospholipid vesicles (C), and purified receptor that had been reconstituted into phospholipid vesicles and subsequently dissolved in 0.86% digitonin (D). Extract from uninfected cells was used as a control (E). In each case, samples cross-linked with BS^3 (lanes 2) and untreated controls (lanes 1) were prepared in parallel. Lanes 1 and 2 in each panel received the same amount of receptor, as determined from the binding of [^{3}H]QNB (15−25 fmol). The data are from three gels as follows: panel A, panels B and C, and panels D and E. The area under the densitometric trace was determined in four segments as shown in panels A, B, and D (*a*, 40−75 kDa; *b*, 75−170 kDa; *c*, 170−360 kDa; and *d*, >360 kDa), and the relative contribution of each segment to the total intensity is listed in Table 1. Panels A and B are representative of the results from at least four batches of solubilized and purified receptor. Panel C is representative of the results from five independent reconstitutions performed with three different batches of purified receptor (i.e., 1, 2, and 2 reconstitutions per batch). When a reconstitution was followed by resolubilization, samples were taken from both preparations. Blots from three batches of purified receptor and three to five independent reconstitutions were analyzed to obtain the values listed in Table 1.

dx.doi.org/10.1021/bi4003869 | *Biochemistry* 2013, 52, 7405−7427

Table 1. Distribution of the M_2 Receptor among the Monomeric and Oligomeric States Identified on Western Blots[a]

receptor	BS^3	NEM	intensity (%)			
			a	*b*	*c*	*d*
unprocessed extract	− (3)	−	40 ± 1	44 ± 5	16 ± 4	
	+ (3)	−	6 ± 3	6 ± 2	40 ± 6	48 ± 2
purified	− (5)	−	96 ± 2	4 ± 2		
	+ (6)	−	79 ± 5	10 ± 3	11 ± 2	
purified and reconstituted	− (5)	−	89 ± 5	11 ± 5		
	+ (5)	−			44 ± 8	56 ± 8
purified, reconstituted, and resolubilized	− (2)	−	82 ± 12	18 ± 12		
	+ (3)	−	7 ± 6	2 ± 2	56 ± 5	35 ± 4
purified	− (4)	+	79 ± 18	21 ± 18		
	+ (4)	+	64 ± 8	10 ± 2	26 ± 5	
purified and reconstituted	− (2)	+	94 ± 6	6 ± 6		
	+ (2)	+			32 ± 14	68 ± 14

[a]The area under the densitometric trace from each lane of Western blots such as those illustrated in Figures 2 and 7 was estimated in four segments corresponding roughly to monomers (*a*), dimers and trimers (*b*), and larger aggregates (*c* and *d*), as described in the legend of Figure 2. Each value was expressed as a percentage of the total area for that lane, and the values from different blots were averaged to obtain the means (±SEM) listed in the table. The number of blots is shown in parentheses. In each case, the time of exposure was selected to avoid overexposure of the film. Further details are described in the legends of Figures 2 and 7.

Scheme 3 depicts a divalent receptor, presumably a monomer, with one orthosteric site and one allosteric site. Ligands P and A compete for the orthosteric site of an otherwise vacant receptor with equilibrium dissociation constants K_{Po} and K_{Ao}, respectively. Ligand A also binds to the allosteric site with dissociation constant K_{Aa}. The parameter α is the cooperativity factor for the interaction between P at the orthosteric site and A at the allosteric site; similarly, β is the cooperativity factor for interaction between A at the orthosteric site and A at the allosteric site. The total specific binding of the probe was calculated according to eq 6, in which $B_{sp} = [RP] + [ARP]$. Variables [P] and [A] represent the free concentrations of the two ligands, which were essentially the same as the total concentrations under the conditions of the assays (i.e., $0.99[L]_t < [L] < [L]_t$).

$$B_{sp} = \left[[R]_t \frac{[P]}{K_{Po}}\left(1 + \frac{[A]}{\alpha K_{Aa}}\right)\right] \Big/ \left[1 + \frac{[A]}{K_{Aa}} + \frac{[A]}{K_{Ao}}\left(1 + \frac{[A]}{\beta K_{Aa}}\right) + \frac{[P]}{K_{Po}}\left(1 + \frac{[A]}{\alpha K_{Aa}}\right)\right] \quad (6)$$

Most analyses involved multiple sets of data, and each set generally was assigned separate values of B_{max} and NS (eq 1), $B_{[A]=0}$ and $B_{[A]\to\infty}$ (eqs 2 and 3), or $[R]_t$ and NS (Schemes 1−3). The values of other parameters were shared as described in the figures and tables. To present the results of such analyses, the measured values of B_{obsd} from individual experiments were normalized in the context of the fitted model as described previously (eq 6 of ref 49); normalized estimates of specific binding were averaged to obtain the means plotted on the *y*-axis. All parameters were estimated by nonlinear regression. Equilibrium constants and cooperativity factors were optimized throughout on a logarithmic scale. The data were weighted according to the measured estimate of the standard error on each point. Arithmetic means are presented together with the standard error. Parametric values derived from a single analysis of one or more sets of data are presented together with the errors as estimated from the covariance matrix. Differences in the goodness of fit were assessed throughout by means of the *F*-statistic. Linear correlations were performed using GraphPad (Prism 3.03). Other details regarding the analyses and statistical procedures have been described previously (ref 50 and references cited therein).

RESULTS

Reconstitution of Oligomers. HA- and FLAG-tagged M_2 muscarinic receptors were co-expressed in *Sf*9 cells and purified by successive passage on DEAE-Sepharose, aminobenztropine-Sepharose, and hydroxyapatite. Western blots of the unprocessed extract revealed a mixture of species (Figure 2A, lane 1). Densitometric analyses indicated that 40% of the immunoreactive material migrated as a doublet with apparent molecular masses expected of a monomer [i.e., 47 ± 4 kDa ($N = 2$) and 54 ± 3 kDa ($N = 3$)] (Table 1). The balance migrated more slowly in the manner expected of a dimer [126 ± 12 kDa, 44% ($N = 3$)] and a tetramer [226 ± 16 kDa, 16% ($N = 3$)]. The monomeric fraction was reduced to 6% after treatment with BS^3, while 88% migrated with an apparent molecular mass of ≥255 ± 27 kDa ($N = 3$) (Figure 2A, lane 2; Table 1). These observations suggest that M_2 receptors exist predominantly as oligomers in unprocessed extracts of *Sf*9 cells. That preparation therefore served as a positive control for cross-linking and co-immunoprecipitation. The efficiency of co-immunoprecipitation was 51% for receptors bearing the HA and FLAG epitopes (Figure S2 of the Supporting Information, lanes 1 and 2).

The purified receptor was largely monomeric, as observed previously.[50,51,54] Ninety-six percent of the immunoreactive material migrated as a doublet with apparent molecular masses of 45 ± 2 and 51 ± 2 kDa ($N = 7$); the balance migrated as a faint band with an apparent molecular mass approximating that of a dimer [i.e., 123 ± 7 kDa ($N = 7$)] (Figure 2B, lane 1; Table 1). The predominantly monomeric status of the purified receptor was confirmed in part by the small effect of BS^3 in those preparations, where bands corresponding to monomers accounted for 79% of the total intensity after cross-linking (Figure 2B, lane 2; Table 1); also, the efficiency of co-immunoprecipitation of the HA and FLAG epitopes was only 5% after purification, or 10-fold less than the value of 51% obtained with unprocessed extracts (Figure S2 of the Supporting Information, lanes 1−4).

dx.doi.org/10.1021/bi4003869 | *Biochemistry* 2013, 52, 7405−7427

The purified M_2 receptor was reconstituted into phospholipid vesicles, and the intensity-based distribution of hydrodynamic sizes was determined by dynamic light scattering (Figure 3).

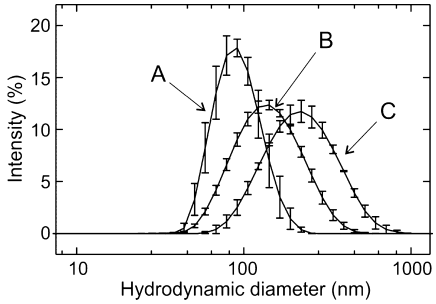

Figure 3. Characterization of vesicular size and homogeneity. Vesicles of POPC, POPS, and cholesterol were characterized by dynamic light scattering, with three or more traces recorded for each of one to six independent preparations. The intensities in each bin were averaged over all traces, and the means from the different preparations were averaged to obtain the mean of means (±SEM) plotted on the *y*-axis. The fitted estimates of the average hydrodynamic size (*Z*-average) and the polydispersity index for the different traces and different preparations were averaged in a similar manner, and the mean values are as follows: vesicles alone (A), 87.6 ± 6.4 nm and 0.080 ± 0.009 (N = 3), respectively; vesicles with receptors (B), 127 ± 5 nm and 0.17 ± 0.02 (N = 6), respectively; vesicles with receptors and G proteins (C), 190 ± 2 nm and 0.20 ± 0.01 (N = 1), respectively.

Vesicles lacking receptor and G protein gave a mean value of 88 nm for the average hydrodynamic diameter and a mean polydispersity index of 0.080. Upon incorporation of the detergent-solubilized purified receptor, the distribution shifted to somewhat larger sizes and broadened, as indicated by an increase in the average hydrodynamic diameter to 127 nm and in the polydispersity index to 0.17. Upon the incorporation of purified receptor and G proteins in one preparation, the average hydrodynamic diameter increased to 190 nm with a polydispersity index of 0.20. The symmetry of the intensity distributions and the low to moderate polydispersity indices ($\leq$0.2) suggest that large or poorly defined aggregates did not occur to an appreciable extent.

Detergent alone affected neither the diameter nor the polydispersity index when added at a concentration equal to that in the preparation of purified receptor. The diameter increased at higher concentrations but in a saturable manner, and the asymptotic value of ~110 nm was smaller than the diameter of vesicles loaded with receptor (Figure S1 of the Supporting Information).

Taken without cross-linking, the reconstituted receptor migrated primarily as a monomer on denaturing polyacrylamide gels, where 89% of the densitometric intensity corresponded to apparent molecular masses of 46 ± 2 and 51 ± 2 kDa (N = 7) (Figure 2C, lane 1; Table 1). The balance corresponded to a dimer [118 ± 6 kDa (N = 8)]. When the reconstituted sample was reacted with BS^3 prior to electrophoresis, most of the immunoreactive material migrated as a single band with an apparent molecular mass of 256 ± 12 kDa (N = 8) (Figure 2C, lane 2; Table 1). Also, reconstitution increased the efficiency of co-immunoprecipitation of the HA and FLAG epitopes to 43% (Figure S2 of the Supporting Information, lanes 5 and 6), which compares favorably with the value of 51% obtained with unprocessed extracts. Monomers of the M_2 receptor therefore appeared to reassociate in phospholipid vesicles, forming aggregates with the electrophoretic mobility of tetramers or pentamers.

To examine the stability of newly formed oligomers, vesicles containing the reconstituted receptor were solubilized in 0.86% digitonin prior to electrophoresis. With no cross-linking, 82% of the reconstituted and resolubilized receptor migrated as a monomer (Figure 2D, lane 1). Treatment with BS^3 after resolubilization reduced the complement of monomers to 7%, and most of the receptor migrated as a tetramer [219 ± 10 kDa (N = 3)] or larger aggregates (Figure 2D, lane 2; Table 1). These observations indicate that oligomers formed upon reconstitution of the M_2 receptor with synthetic lipids were sufficiently stable to survive solubilization in digitonin. A similar stability was observed previously in the case of tetramers that formed when differently tagged monomers of the M_2 receptor were reconstituted with lipids from natural sources. After resolubilization in digitonin, the receptors showed a high degree of co-immunoprecipitation and, when cross-linked with BS^3, migrated predominantly as tetramers.[50]

BS^3 was saturating at the usual concentration of 2 mM, both in the reconstituted preparation and after resolubilization (Figure S3 of the Supporting Information). At that concentration, monomers typically were absent from Western blots of the reconstituted preparation (Figure 2 and Figure S3 of the Supporting Information). Monomers appeared as a minor component when receptors were cross-linked after resolubilization, but they represented the same fraction of the total density at BS^3 concentrations from 1 to 8 mM (Figure S3 of the Supporting Information). The relative densities of the different bands therefore appear to indicate the amounts of monomeric and oligomeric species that were present in the original sample. BS^3 increased slightly the mobility of the monomeric band when that band could be compared before and after treatment (e.g., Figure 2B, lane 2; Figure S3B of the Supporting Information, lanes 6–9). The increase suggests that BS^3 affects the axial ratio of monomers in solution but does not lead to their cross-linked association as dimers or larger oligomers.

To confirm the purity of the receptor, samples processed on DEAE-Sepharose, ABT-Sepharose, and hyproxyapatite in the usual manner were examined by electrophoresis and silver staining (Figure S4 of the Supporting Information). In accord with previous results,[50] a doublet corresponding to monomers of the receptor accounted for 68–69% of the stained protein. Apparent oligomers (3%) and proteolytic products (13–14%) that included a 35 kDa fragment (11%) accounted for an additional 16–17%, as indicated by comparison with Western blots (Figure S4 of the Supporting Information) or by mass spectrometry.[50] The balance of ~15% was distributed among unidentified minor bands, the quantities of which were negligible. All of the immunopositive bands that ran with an apparent molecular mass of $\lesssim$50 kDa were absent after cross-linking with BS^3, even after a lengthy exposure of the film. The disappearance suggests either that the 35 kDa fragment and other proteolytic products copurified as a viable receptor later stabilized by cross-linking[51] or that cross-linking prevented proteolysis that otherwise occurred during preparation of the sample for electrophoresis.

Binding to Reconstituted Oligomers. When assembled with G proteins in vesicles of POPC, POPS, and cholesterol, the purified M_2 receptor bound agonists in the manner described previously for muscarinic and other GPCRs in native membranes and reconstituted preparations (e.g., refs 13, 35, 46, and 50). The specific binding of *N*-[^{3}H]methylscopolamine was inhibited by

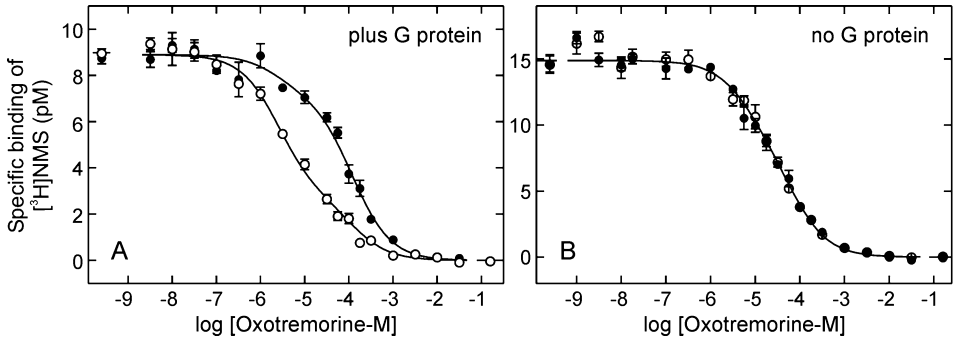

Figure 4. Effect of GMP-PNP on the binding of oxotremorine-M to purified M_2 receptor reconstituted with (A) and without (B) G proteins. The molar ratio of receptor to G proteins during reconstitution was 1:10. Total binding was measured at a subsaturating concentration of [^{3}H]NMS (A, 14.1 ± 0.6 nM; B, 5.4 ± 0.3 nM) and graded concentrations of oxotremorine-M. Assays in the absence of guanylyl nucleotide (○) and in the presence of 0.1 mM GMP-PNP (●) were conducted in parallel. The lines in each panel depict the best fit of eq 3 (n = 2) to the data from three (A) or four (B) experiments taken in concert. For the analysis represented in panel A, single values of log $IC_{50(j)}$ were common to all of the data, and separate values of F_j were assigned to data acquired in the absence or presence of GMP-PNP; the sum of squares was not significantly higher than that obtained with separate values of log $IC_{50(j)}$ for data acquired with and without the nucleotide (P = 0.085). For the analysis represented in panel B, single values of log $IC_{50(j)}$ and F_j were common to all of the data irrespective of GMP-PNP; the sum of squares was not significantly higher than that obtained with separate values of each parameter for data acquired with and without the nucleotide (P = 0.25). The fitted parametric values are as follows: (A) log $IC_{50(H)}$ = −5.59 ± 0.09, log $IC_{50(L)}$ = −3.92 ± 0.06, and F_H = 0.68 ± 0.04 (no GMP-PNP) or 0.18 ± 0.05 (plus GMP-PNP); (B) log $IC_{50(H)}$ = −5.15 ± 0.14, log $IC_{50(L)}$ = −4.19 ± 0.12, and F_H = 0.39 ± 0.14 (±GMP-PNP). The mean values of $B_{[A]=0}$ that were used to obtain the adjusted values of B_{sp} plotted on the y-axis are 9.0 ± 1.0 pM (A; N = 6) and 15.0 ± 2.9 pM (B; N = 8).

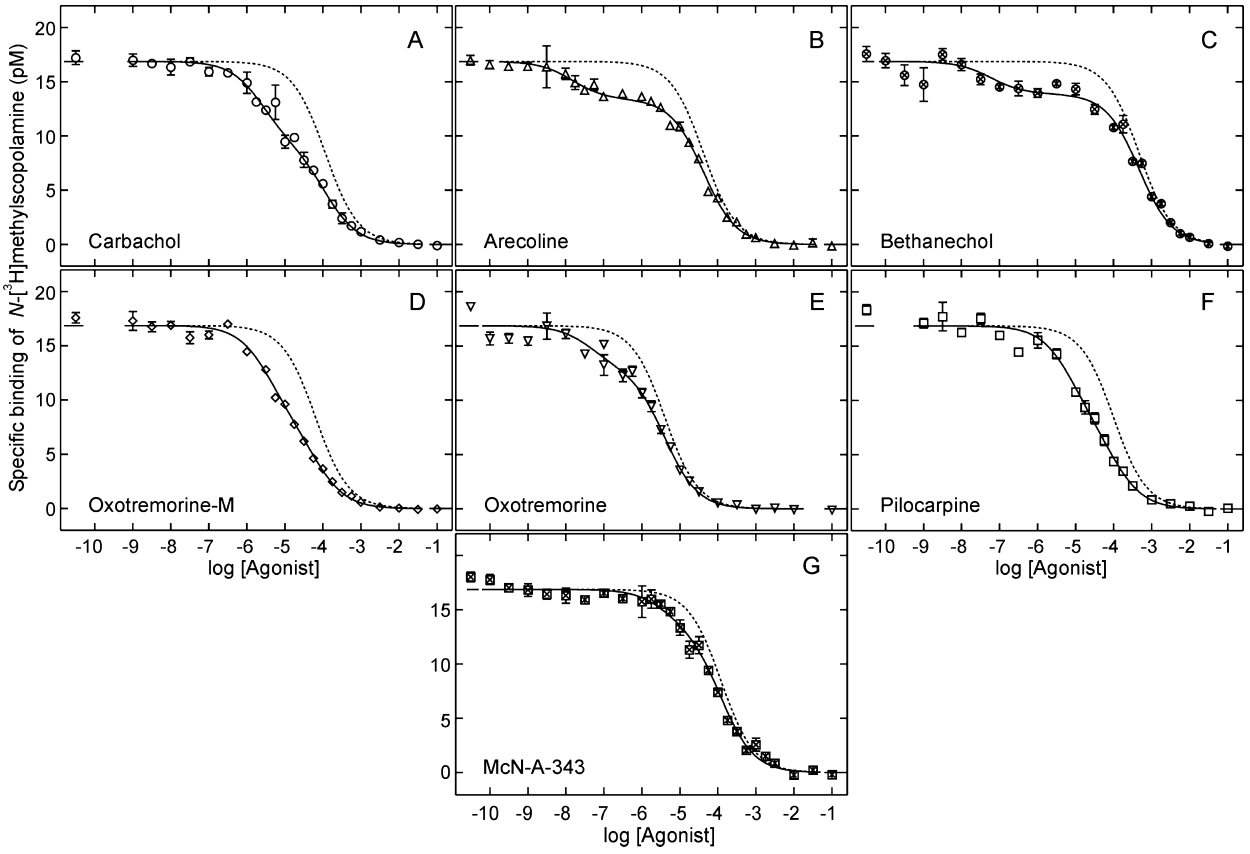

Figure 5. Binding of agonists to purified M_2 receptor reconstituted without G proteins. Total binding was measured at a half-saturating concentration of [^{3}H]NMS (5.27 ± 0.06 nM) and graded concentrations of unlabeled carbachol (A), arecoline (B), bethanechol (C), oxotremorine-M (D), oxotremorine (E), pilocarpine (F), or McN-A-343 (G). The solid line in each panel represents the best fit of eq 3 (n = 2) to the data from four to eight experiments taken in concert, and the fitted parametric values are listed in Table 2. In each case, the sum of squares was significantly lower with two classes of sites than with one as determined by the F-statistic ($P \leq 0.00007$). The dotted line in each panel depicts the simulated curve for a single class of sites with a value of IC_{50} equal to the value of $IC_{50(L)}$ obtained from the fit of eq 3 (n = 2) to the experimental data. The mean value of $B_{[A]=0}$ for the 56 sets of data represented in this figure and Figure 6 was used to obtain the adjusted values of B_{sp} plotted on the y-axis (i.e., 17.1 ± 1.2 pM).

oxotremorine-M to reveal a dispersion of affinities (Figure 4A) characterized by a Hill coefficient of 0.60 ± 0.04 and an overall potency of 7.2 μM (log IC_{50} = −5.14 ± 0.06) (eq 2). Upon inclusion of GMP-PNP, the Hill coefficient increased to 0.77 ±

dx.doi.org/10.1021/bi4003869 | Biochemistry 2013, 52, 7405−7427

Table 2. Parametric Values for the Binding of Ligands to the Reconstituted M_2 Receptor[a]

ligand[b]	eq 2; n_H	eq 3			
		log $IC_{50(H)}$	log $IC_{50(L)}$	F_H	potential shift (Δlog $IC_{50} \times F_H$)
agonists					
1. carbachol (6)	0.59 ± 0.04	−5.60 ± 0.17	−3.94 ± 0.11	0.45 ± 0.06	0.75 ± 0.09
2. arecoline (5)	0.73 ± 0.04	−7.82 ± 0.19	−4.37 ± 0.03	0.21 ± 0.02	0.71 ± 0.08
3. bethanechol (6)	0.71 ± 0.04	−7.23 ± 0.27	−3.33 ± 0.04	0.18 ± 0.02	0.69 ± 0.10
4. oxotremorine-M (8)	0.69 ± 0.02	−5.42 ± 0.09	−4.20 ± 0.09	0.52 ± 0.06	0.64 ± 0.07
5. oxotremorine (4)	0.74 ± 0.04	−7.34 ± 0.31	−5.40 ± 0.06	0.23 ± 0.04	0.44 ± 0.07
6. pilocarpine (5)	0.72 ± 0.03	−5.13 ± 0.17	−4.00 ± 0.16	0.51 ± 0.12	0.58 ± 0.13
7. McN-A-343 (5)	0.79 ± 0.04	−5.40 ± 0.34	−3.92 ± 0.06	0.19 ± 0.06	0.29 ± 0.05
antagonists					
8. quinuclidinylbenzilate (4)[c]	1.02 ± 0.07	−9.54 ± 0.04			0
9. *N*-methylscopolamine (5)[c]	0.96 ± 0.08	−8.21 ± 0.04			0
10. atropine (8)	0.81 ± 0.03	−9.31 ± 0.25	−7.53 ± 0.04	0.15 ± 0.03	0.27 ± 0.04

[a]The data represented in each panel of Figures 5 and 6 were analyzed in terms of the Hill equation (eq 2) and as a sum of hyperbolic terms (eq 3; n = 1 or 2) to obtain the parametric values listed here. Single values of log IC_{50} and n_H (eq 2) and of log $IC_{50(j)}$ and F_j (eq 3) were common to the data from all experiments included in the analysis. The number of experiments is shown in parentheses. Further details are described in the legends of Figures 5 and 6. [b]The numbering of ligands corresponds to that in Table 5, Figure 13, and Table S5 and Figure S11 of the Supporting Information. [c]The value of n_H is indistinguishable from 1 ($P \geq 0.61$), and one term is sufficient for eq 3 to describe the data ($P \geq 0.84$).

0.05, and the value of IC_{50} increased 11-fold to 76 μM (log IC_{50} = −4.12 ± 0.05) (eq 2). If the data are described as a sum of two hyperbolic terms (eq 3), the effect of GMP-PNP was to cause an apparent interconversion of sites from higher to lower affinity for the agonist (Figure 4A); that is, the fraction of high-affinity sites decreased from 0.68 to 0.18 with no change in the value of $IC_{50(j)}$ of either class. Binding at graded concentrations of *N*-[^{3}H]methylscopolamine alone revealed a dispersion of affinities for the radioligand (n_H = 0.66 ± 0.04, log EC_{50} = −7.70 ± 0.10, eq 1, N = 3), but there was no change upon addition of GMP-PNP (Table S1 of the Supporting Information).

The purified M_2 receptor also appeared to be heterogeneous when reconstituted without G proteins (Figure 5). Seven full and partial agonists inhibited the specific binding of *N*-[^{3}H]-methylscopolamine with Hill coefficients significantly less than 1 ($P \leq 0.00001$) (Table 2). In each case, two classes of sites are required to describe the data in terms of eq 3 ($P \leq 0.00007$); the fitted curves are illustrated in Figure 5, and the parametric values are listed in Table 2. Also shown for each agonist in Figure 5 is the simulated curve for the pattern that would be obtained if all of the high-affinity sites were converted to low affinity. That approximates the effect of GTP and analogues such as GMP-PNP in G protein-containing preparations, and it therefore represents the potential for such an effect in preparations without G protein. The magnitude is given by the quantity $F_H \times \Delta$log IC_{50} (Table 2), which equals the area between the two curves as described in Materials and Methods (Figure 1) and the Supporting Information.

There was no effect of GMP-PNP on the binding of oxotremorine-M to receptor reconstituted in the absence of G protein (Figure 4B). Also, the pattern of inhibition by carbachol was unchanged after periods of incubation from 30 min to 3 h (Figure S5 of the Supporting Information), indicating that the system had attained equilibrium under the conditions of the binding assays.

The antagonists quinuclidinylbenzilate and *N*-methylscopolamine inhibited the specific binding of *N*-[^{3}H]-methylscopolamine with Hill coefficients indistinguishable from 1, and one class of sites is sufficient to describe the data in terms of eq 3 (Figure 6A,B and Table 2). Atropine gave a Hill coefficient significantly less than 1 ($P < 0.00001$) [n_H = 0.81 (Table 2)], and two classes of sites are required with eq 3 ($P < 0.00001$) (Figure 6C and Table 2). Binding at graded concentrations of *N*-[^{3}H]methylscopolamine alone revealed a Hill coefficient near 1 and an apparent affinity that was ∼6-fold higher than that measured in the presence of G proteins (n_H = 0.90 ± 0.02, log EC_{50} = −8.45 ± 0.02, eq 1; N = 7) (Table S1 of the Supporting Information).

Effects of *N*-Ethylmaleimide on Binding to Reconstituted Oligomers. To compare the heterogeneity revealed by agonists and the inverse agonist atropine, the distribution of reconstituted receptors between active and inactive states was shifted using *N*-ethylmaleimide.[48] With the purified receptor in solution, alkylation reduced the complement of monomers detected after cross-linking with BS^3 from 79% of the immunoreactive material to 64%; the complement of dimers was unchanged at 10%, and that of tetramers and larger oligomers increased from 11 to 26% (Figure 7A, lanes 2 and 4; Table 1). With the reconstituted receptor, monomers and smaller oligomers were absent from cross-linked preparations irrespective of *N*-ethylmaleimide; the complement of tetramers was reduced from 44 to 32% with a concomitant increase in that of larger aggregates, although this effect was not statistically significant (P = 0.49) (Figure 7B, lanes 2 and 4; Table 1). Alkylation therefore had comparatively little effect on the oligomeric status of the purified receptor, which remained predominantly monomeric in solution and wholly oligomeric after reconstitution.

Treatment of the reconstituted receptor with *N*-ethylmaleimide decreased the apparent affinity of *N*-[^{3}H]-methylscopolamine ∼33-fold in terms of eq 1 (Figure 8A), and the corresponding Hill coefficient decreased from 0.90 to 0.61 (Table S1 of the Supporting Information). The inhibitory potency of atropine decreased ∼2.4-fold in terms of eq 2 (Figure 8B). In contrast, the inhibitory potency of oxotremorine-M increased 4.0-fold (Figure 8B). Both unlabeled ligands gave Hill coefficients significantly less than 1 before and after treatment with *N*-ethylmaleimide (legend of Figure 8). Treatment with *N*-ethylmaleimide reduced the capacity for *N*-[^{3}H]-methylscopolamine by ∼40%, which has been shown previously to result from the comparative instability of the alkylated receptor.[48]

dx.doi.org/10.1021/bi4003869 | *Biochemistry* 2013, 52, 7405−7427

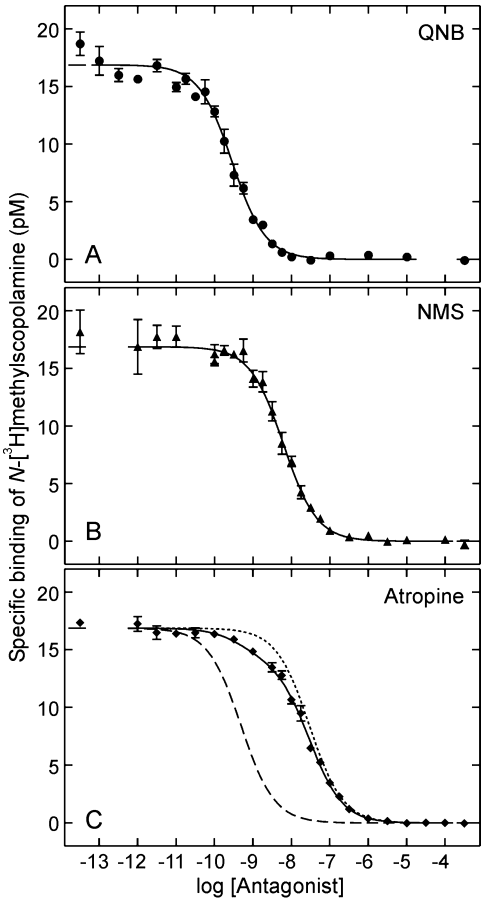

Figure 6. Binding of antagonists to purified M_2 receptor reconstituted without G proteins. Total binding was measured at a half-saturating concentration of [^{3}H]NMS (5.17 ± 0.12 nM) and graded concentrations of unlabeled QNB (A), NMS (B), or atropine (C). The solid line in each panel depicts the best fit of eq 3 (n = 1 or 2) to the data from four to eight experiments taken in concert, and the fitted parametric values are listed in Table 2. One class of sites was sufficient for QNB and NMS ($P \geq 0.84$). In the case of atropine, the sum of squares was significantly lower with two classes of sites than with one ($P < 0.00001$). The dotted and dashed lines in panel C depict the simulated curves for a single class of sites with an IC_{50} value equal to the value of $IC_{50(L)}$ and $IC_{50(H)}$, respectively, obtained from the fit of eq 3 to the experimental data (n = 2). The mean value of $B_{[A]=0}$ for the 56 sets of data represented in Figure 5 and this figure was used to obtain the adjusted values of B_{sp} plotted on the y-axis (i.e., 17.1 ± 1.2 pM).

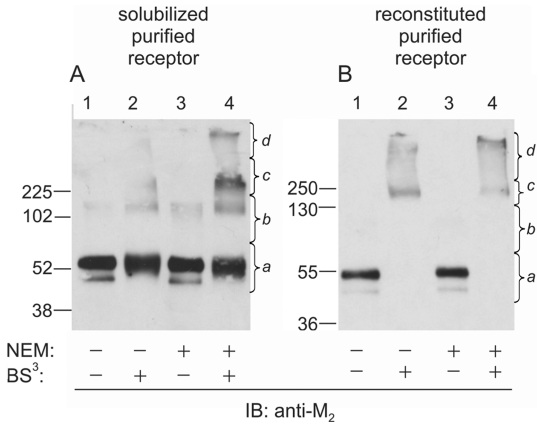

Figure 7. Electrophoretic mobility of purified M_2 receptor treated with N-ethylmaleimide. Samples of the receptor in solution (A) and after reconstitution (B) were treated with BS^3 (lanes 2), with NEM (lanes 3), or with NEM and subsequently with BS^3 (lanes 4). Untreated samples were taken as controls (lanes 1). All lanes contained the same amount of receptor, as determined from the binding of [^{3}H]QNB (15−25 fmol). The area under the densitometric trace was measured in four segments (cf. Figure 2, a−d), and the relative contribution of each segment to the total intensity is listed in Table 1.

To rationalize the heterogeneity reflected in the low values of n_H, the data represented in both panels of Figure 8 were analyzed in terms of Scheme 1 (eq 4). The effects of N-ethylmaleimide were assigned wholly to changes in F_j, each of which was taken as the same for all ligands. It was assumed that N-ethylmaleimide was without effect on any value of K_{Pj} or K_{Aj}. These constraints increased the global sum of squares with two classes of sites ($P < 0.00001$) but had no appreciable effect with three classes ($P = 0.090$). The parametric values for three classes of sites are listed in Table 3, and the fitted curves are shown in Figure 8. Although the origin of the heterogeneity is not explicit in Scheme 1, this assignment of parameters implies that alkylation affects the distribution of receptors among the different states without affecting affinity per se.

The three classes of receptor showed the opposite preference for agonists and antagonists: that is, the sites of higher affinity for the former were of lower affinity for the latter and vice versa (Table 3). Whereas native receptors were wholly in the states of lower affinity for oxotremorine-M and higher affinity for atropine and N-[^{3}H]methylscopolamine (i.e., $F_2 + F_3 > 0.99$), those treated with N-ethylmaleimide were primarily in the state of highest affinity for oxotremorine-M and lowest affinity for atropine and N-[^{3}H]methylscopolamine ($F_1 = 0.75$). The heterogeneity displayed by reconstituted M_2 receptors therefore was affected in a manner that mimicked the effect of N-ethylmaleimide on M_2 receptors in membranes and purified preparations from porcine atria.[48,55,56] Essentially the same result was obtained from a similar analysis in terms of two classes of sites rather than three, but the sum of squares was significantly higher ($P < 0.00001$) (Figure S6 and Table S2 of the Supporting Information).

The difference in the effect of N-ethylmaleimide on the binding of agonists and antagonists suggests that the heterogeneity revealed in the binding assays is not directly comparable across both classes of ligand. If the potential effect of GTP on the binding of agonists is the area defined by a virtual interconversion of sites from higher to lower affinity, as illustrated by the dotted lines in Figure 5 [i.e., the product of $\Delta\log IC_{50}$ and F_H (Table 2)], it follows that the corresponding effect for antagonists is the area defined by a virtual interconversion from lower to higher affinity, as illustrated by the dashed line in Figure 6C (i.e., the product of $\Delta\log IC_{50}$ and F_L).

Origin of Heterogeneity within an Oligomer. Heterogeneity revealed in the binding of a ligand to a homotetramer implies asymmetry, either intrinsic to the oligomeric state or induced as a consequence of cooperativity between interacting sites.[57] A constitutively asymmetric system devoid of cooperative effects is equivalent to Scheme 1 with n classes of mutually independent sites, each of which accounts for the fraction $1/n$ of the total number of protomers. Binding in such a system is strictly competitive, which can be distinguished from cooperativity by comparing the affinity of a radioligand measured directly with that inferred from the inhibitory effect of an unlabeled ligand.[58] The binding of N-methylscopolamine therefore was

dx.doi.org/10.1021/bi4003869 | Biochemistry 2013, 52, 7405−7427

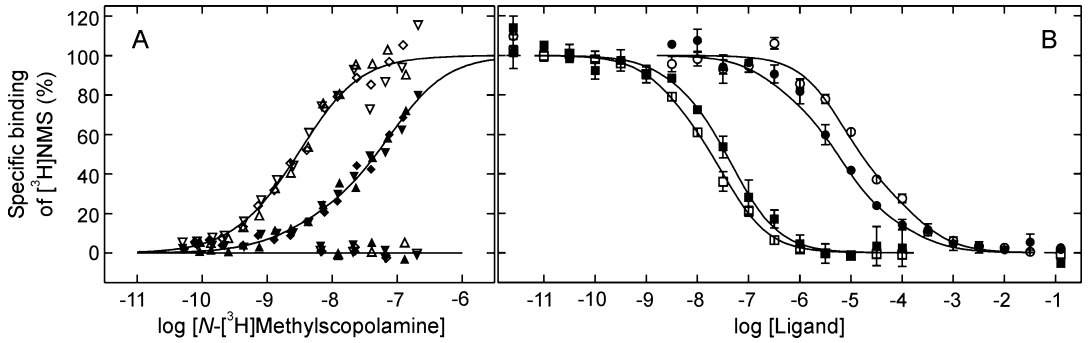

Figure 8. Effect of *N*-ethylmaleimide on the binding of oxotremorine-M, atropine, and *N*-methylscopolamine to the reconstituted M_2 receptor. Assays of the receptor before (empty symbols) and after (filled symbols) treatment with NEM were conducted in parallel. (A) Total binding was measured at graded concentrations of [^{3}H]NMS, either alone (top curves) or in the presence of 1 mM unlabeled NMS (baseline). The results from three experiments are shown, and different symbols denote data from different experiments (△ and ▲, ▽ and ▼, or ◇ and ◆). (B) Total binding was measured at a subsaturating concentration of [^{3}H]NMS (5.15 ± 0.06 nM) and graded concentrations of oxotremorine-M (○ and ●) or atropine (□ and ■). The results of three experiments are shown for each ligand. The lines depict the best fit of Scheme 1 (eq 4; $n = 3$) to the pooled data from the nine experiments represented in both panels. The fitted values of log K_{Lj} and F_j are listed in Table 3. The mean values of $[R]_t$ for untreated and NEM-treated receptor are 14.5 ± 0.9 and 8.72 ± 0.87 pM ($N = 9$), respectively. The adjusted values of B_{sp} were normalized to the maximum taken as 100 to obtain the values plotted on the *y*-axis. The data also were analyzed in terms of the Hill equation (eq 1 or 2), and the fitted estimates of potency (log EC_{50} or log IC_{50}) and n_H are as follows: (A, [^{3}H]NMS) −8.53 ± 0.04 and 0.90 ± 0.05 (without NEM) and −7.02 ± 0.27 and 0.61 ± 0.06 (with NEM), respectively; (B, atropine) −7.76 ± 0.03 and 0.79 ± 0.04 (without NEM) and −7.37 ± 0.08 and 0.74 ± 0.10 (with NEM), respectively; (B, oxotremorine-M) −4.78 ± 0.04 and 0.71 ± 0.03 (without NEM) and −5.38 ± 0.11 and 0.67 ± 0.10 (with NEM), respectively.

Table 3. Parametric Values for the Effect of *N*-Ethylmaleimide on Binding to the Reconstituted M_2 Receptor[a]

ligand	NEM	log K_{L1}	log K_{L2}	log K_{L3}
oxotremorine-M	±	−6.57 ± 0.61	−5.53 ± 0.07	−4.67 ± 0.20
atropine	±	−7.00 ± 0.38	−7.75 ± 0.11	−9.43 ± 0.21
[^{3}H]NMS	±	−7.07 ± 0.15	−8.37 ± 0.54	−9.14 ± 0.12
	NEM	F_1	F_2	F_3
all ligands	−	0.01	0.76 ± 0.02	0.23 ± 0.05
	+	0.75	0.21 ± 0.04	0.03 ± 0.02

[a]The data represented in both panels of Figure 8 were pooled and analyzed terms of Scheme 1 (eq 4; $n = 3$) to obtain the parametric values listed here. Measurements in the absence and presence of NEM were conducted in parallel, and each experiment was performed three times to obtain the nine sets of data included in the analysis. Single values of F_j were common to all data acquired under the same conditions with respect to NEM, and single values of K_{Lj} were common to all data acquired with each ligand irrespective of NEM (L ≡ A or P). Further details are described in the legend of Figure 8.

measured at graded concentrations of its radiolabeled analogue (Figure 9A), and binding at two concentrations of the radioligand was measured at graded concentrations of two agonists (oxotremorine-M and arecoline) and two inverse agonists (atropine and unlabeled *N*-methylscopolamine) (Figure 9B–D).

A mechanistic assessment of the data represented in Figure 9 requires that the model account for all receptors in the system. It has been shown previously, however, that a subpopulation of M_2 receptors can exhibit anomalously weak affinity for *N*-[^{3}H]-methylscopolamine under some conditions.[50,59] Such an effect is illustrated for *N*-[^{3}H]methylscopolamine and [^{3}H]-quinuclidinylbenzilate in Figure 10, where binding to the purified receptor is compared in the reconstituted preparation and after subsequent dissolution in 0.86% digitonin. The apparent capacity was similar for both radioligands in either preparation (eq 4, $n = 2$, $[R]_{t,[^3H]QNB}/[R]_{t,[^3H]NMS} = 1.1$), notwithstanding the difference in lipophilicity (for *N*-methylscopolamine, log K_{ow} = −2.58; for quinuclidinylbenzilate, log K_{ow} = 3.01),[b] but it was 2.3-fold higher after redissolution. Approximately 50% of the sites therefore appear to be inaccessible or latent when the receptors are located in phospholipid vesicles. The similar capacities for the two radioligands indicate that the shortfall does not arise from sequestration of sites behind a hydrophobic barrier; rather, it appears to be a property of the tetramer. The shortfall in capacity therefore has been attributed to constitutive or induced asymmetry as illustrated in Figure 11.

In the case of constitutive asymmetry (Figure 11A), the inaccessible sites can be disregarded, and binding can be described in terms of Scheme 1 with two classes of equal size (eq 4, $n = 2$, $F_2 = 0.5$). The fitted curves from such an analysis are shown in Figure 9, and the parametric values are listed in Table 4. The data can yield up to four independent estimates of the affinity of *N*-methylscopolamine for each class of sites (i.e., K_{Pj}): one estimate from binding at graded concentrations of the radioligand (Figure 9A) and three estimates from the effect of the radioligand on the inhibitory potencies of unlabeled ligands (Figure 9B–E). It was assumed that the affinities of labeled and unlabeled *N*-[^{3}H]methylscopolamine are the same, and the parameteric values were constrained accordingly (i.e., $K_{Aj} = K_{Pj}$). The values of K_{Pj} listed in Table 4 differ by up to 2.9-fold, and the differences are confirmed by an increase of 14% in the sum of squares when the analysis is repeated with single values of K_{P1} and K_{P2} for all of the data ($P < 0.00001$). Such differences are inconsistent with the model, in which the affinity of *N*-methylscopolamine is expected to be independent of the mode of measurement.

dx.doi.org/10.1021/bi4003869 | *Biochemistry* 2013, 52, 7405–7427

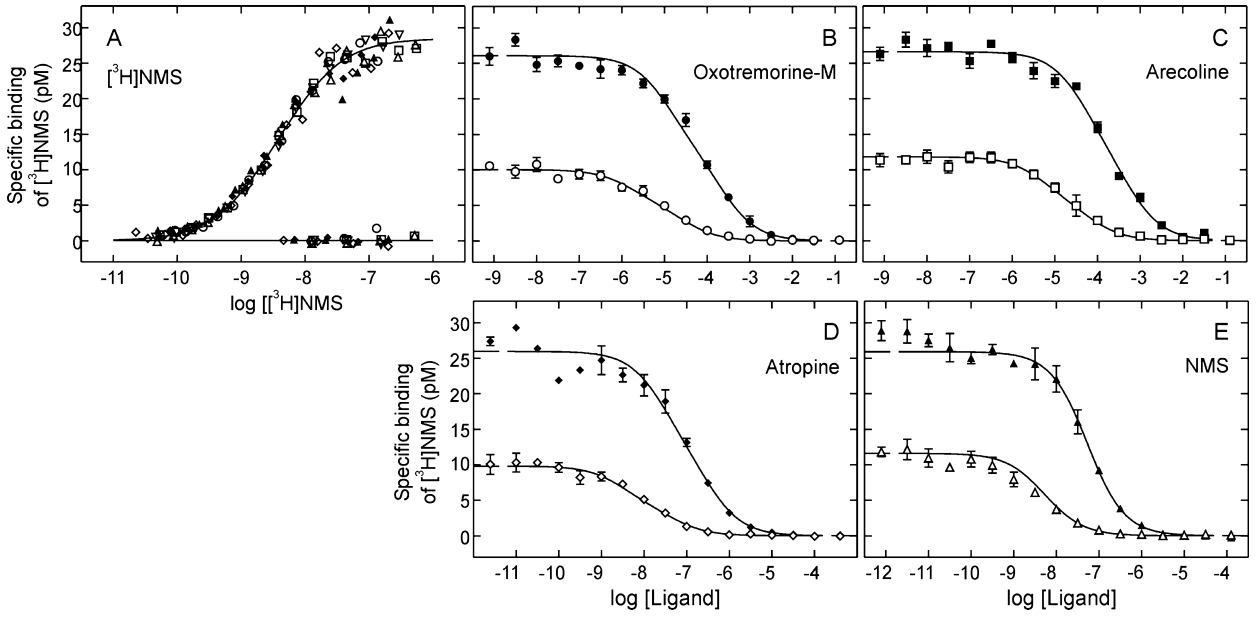

Figure 9. Binding of antagonists and agonists to the reconstituted M_2 receptor, analyzed in terms of a constitutively asymmetric tetramer. (A) Total binding was measured at graded concentrations of [^{3}H]NMS either alone (top curves) or in the presence of 1 mM unlabeled NMS (baseline). Different symbols denote data from seven different experiments. (B–E) Total binding was measured at two concentrations of [^{3}H]NMS [2.45 ± 0.02 nM (empty symbols) and 49.2 ± 0.4 nM (filled symbols)] and graded concentrations of oxotremorine-M (B), arecoline (C), atropine (D), or unlabeled NMS (E). Each experiment included parallel assays at both concentrations of [^{3}H]NMS, and three such experiments were performed with each unlabeled ligand. The lines represent the best fits of Scheme 1 (eq 4, $n = 2$, $F_2 = 0.5$) to the data represented in panels A and E taken in concert and in each of panels B–D. The fitted values of log K_{Aj} and log K_{Pj} are listed in Table 4. The mean value of $[R]_t$ used to obtain the adjusted values of B_{sp} plotted on the y-axis is 28.5 ± 5.2 pM (N = 19). If the labeled sites represent one-half of a tetramer as described in the text, the concentration of tetramers was 14.2 pM.

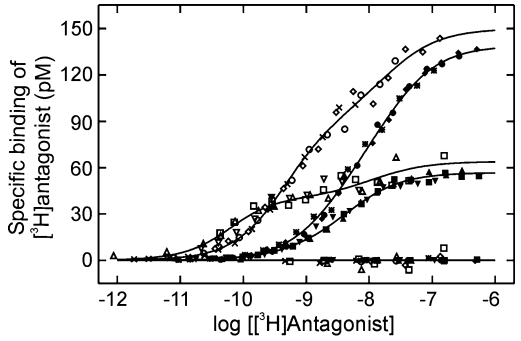

Figure 10. Apparent capacity of reconstituted and resolubilized M_2 receptor for [^{3}H]quinuclidinylbenzilate and N-[^{3}H]methylscopolamine. Purified M_2 receptor was reconstituted in phospholipid vesicles [bottom curves (□, △, ▽, ■, ▲, ▼)], and the reconstituted receptor was resolubilized in 0.86% digitonin [top curves (○, ◇, ×, ●, ◆, ×)]. Total binding was measured at graded concentrations of [^{3}H]QNB (□, △, ▽, ○, ◇, ×) and [^{3}H]NMS (■, ▲, ▼, ●, ◆, ×), either alone or in the presence of 1 mM unlabeled NMS (baseline). The data from three experiments are shown in the figure, and each experiment included assays with both radioligands in both preparations of the receptor. The solid lines represent the best fit of eq 4 (n = 2) to the data from all experiments taken in concert, with single values of log K_{Pj} and F_2 for each radioligand in each preparation. The value of $[R]_t$ was estimated separately for each set of data, and the means were used to obtain the adjusted values of B_{sp} plotted on the y-axis. The values for the reconstituted preparation are as follows: [^{3}H]QNB, 64 ± 22 pM; [^{3}H]NMS, 57 ± 17 pM. The values after resolubilization are as follows: [^{3}H]QNB, 150 ± 20 pM; [^{3}H]NMS, 139 ± 24 pM.

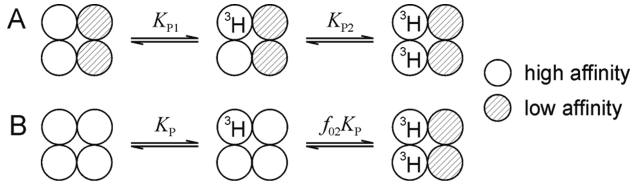

Figure 11. Asymmetry within a tetrameric receptor. (A) Constitutive asymmetry. Two sites of a vacant tetramer are of anomalously weak affinity for the radioligand and therefore inaccessible under the conditions of the assay. The constituent protomers are functionally independent, and the binding of all ligands is strictly competitive. (B) Ligand-induced asymmetry. All sites of a vacant tetramer are of equal affinity for the radioligand. Negative cooperativity precludes occupancy of more than two sites under the conditions of the assays, and cooperativity accounts in part for the inhibitory effect of unlabeled ligands.

In the case of cooperative effects within an otherwise symmetric tetramer (Figure 11B), the latent sites cannot be disregarded because of the different relationships between microscopic and macroscopic affinities in oligomers of different sizes. It therefore was assumed that negative cooperativity prevented occupancy of the tetramer by >2 equiv of the radioligand (i.e., $f_{03} = 10^4$ and $f_{04} = 1$ in Scheme 2). The result is illustrated in Figure S7 of the Supporting Information, where the fitted curves were obtained according to Scheme 2 with the parameters assigned in a mechanistically consistent manner.

The global sum of squares from the unconstrained and mechanistically compromised analysis in terms of Scheme 1 (Figure 9) is the same as that from the mechanistically consistent analysis in terms of Scheme 2 (Figure S7 of the Supporting Information), and both analyses required the same number of parameters. The inability of Scheme 1 to describe the data is indicative of noncompetitive effects, and the agreement with Scheme 2 suggests that the binding patterns are determined at least in part by cooperative interactions.

dx.doi.org/10.1021/bi4003869 | Biochemistry 2013, 52, 7405–7427

Table 4. Parametric Values for the Binding of Ligands at Two Concentrations of *N*-[^{3}H]Methylscopolamine, Analyzed in Terms of Scheme 1[a]

	unlabeled ligand		[^{3}H]NMS	
ligand	log K_{A1}	log K_{A2}	log K_{P1}	log K_{P2}
agonists				
oxotremorine-M (3)	−5.96 ± 0.09	−4.76 ± 0.10	−8.31 ± 0.09	−8.39 ± 0.07
arecoline (3)	−5.52 ± 0.11	−4.42 ± 0.14	−8.49 ± 0.12	−8.44 ± 0.11
antagonists				
atropine (3)	−8.72 ± 0.11	−7.46 ± 0.13	−8.42 ± 0.11	−8.24 ± 0.11
NMS (7, 3)	[−8.77 ± 0.02]	[−8.08 ± 0.04]	−8.77 ± 0.02	−8.08 ± 0.04

[a]The data represented in all panels of Figure 9 were pooled and analyzed in terms of Scheme 1 (eq 4; n = 2) to obtain the parametric values listed here. The value of F_2 was fixed at 0.5. For panels B−D of the figure, single values of log K_{Aj} and log K_{Pj} were common to all data represented in the same panel in obtaining estimates for the unlabeled ligand and [^{3}H]NMS, respectively. For panels A and E of the figure, single values of log K_{Pj} were common to all of the data represented in both panels, and the values of log K_{Aj} for unlabeled NMS were set equal to the corresponding values of log K_{Pj}. The number of experiments is shown in parentheses; in the case of NMS, seven experiments were performed at graded concentrations of the radioligand, and three were performed at graded concentrations of the unlabeled analogue. Further details are described in the legend of Figure 9.

Table 5. Parametric Values for the Binding of Ligands to Purified Monomers of the M_2 Receptor[a]

		eq 3			
ligand[b]	eq 2; n_H	log $IC_{50(H)}$	log $IC_{50(L)}$	F_H	potential shift (Δlog $IC_{50} \times F_H$)
1. carbachol (5)	0.87 ± 0.03	−4.93 ± 0.28	−2.81 ± 0.03	0.12 ± 0.02	0.25 ± 0.03
2. arecoline (7)	0.91 ± 0.03	−4.55 ± 0.49	−3.11 ± 0.04	0.12 ± 0.05	0.17 ± 0.04
4. oxotremorine-M (3)[c]	0.95 ± 0.03	−3.63 ± 0.02			0
5. oxotremorine (5)	0.85 ± 0.02	−5.22 ± 0.03	−3.99 ± 0.05	0.18 ± 0.06	0.22 ± 0.04
6. pilocarpine (4)	0.78 ± 0.03	−3.93 ± 0.11	−2.83 ± 0.10	0.49 ± 0.07	0.54 ± 0.07
7. McN-A-343 (3)	0.84 ± 0.03	−4.09 ± 0.20	−3.19 ± 0.02	0.57 ± 0.19	0.51 ± 0.18
10. atropine (3)[c,d]	1.02 ± 0.04	−7.06 ± 0.02			0

[a]The data represented in each panel of Figure 12 were analyzed in terms of the Hill equation (eq 2) and as a sum of hyperbolic terms (eq 3; n = 1 or 2) to obtain the parametric values listed here. The number of experiments is shown in parentheses. Further details are described in the legend of Figure 12 and the footnotes of Table 2. [b]The numbering of ligands corresponds to that in Table 2, Figure 13, and Table S5 and Figure S11 of the Supporting Information. [c]The value of n_H is not significantly different from 1, and one term is sufficient for eq 3 to describe the data (P > 0.05). [d]The data for atropine are not given.

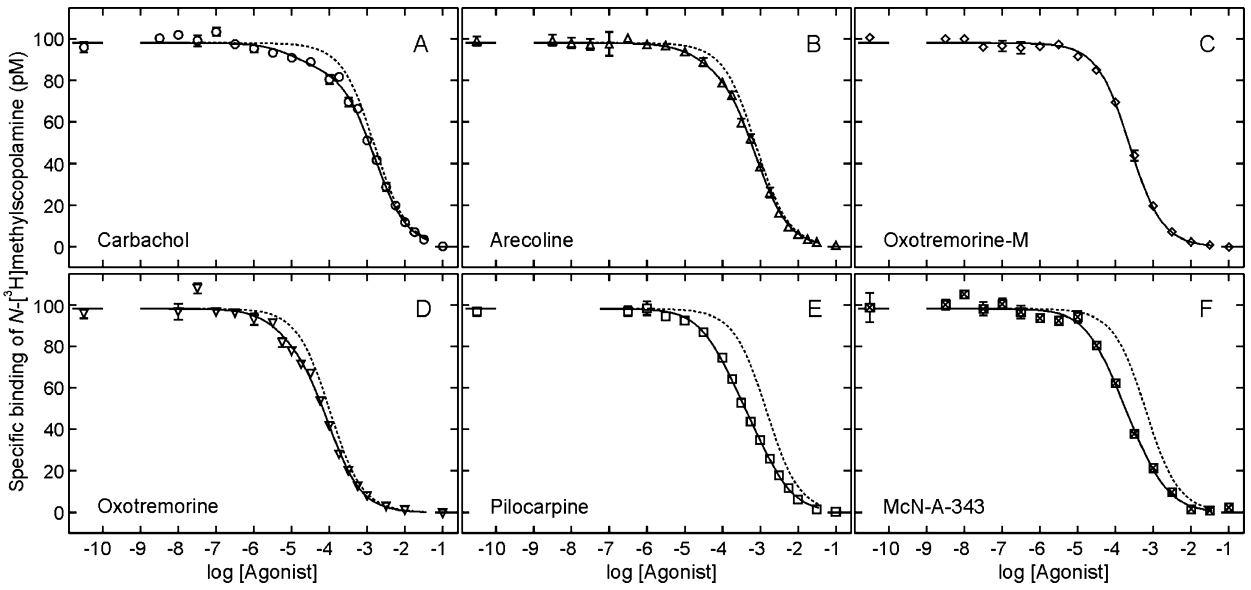

Figure 12. Binding of agonists to purified monomers of the M_2 receptor. Total binding was measured at a half-saturating concentration of [^{3}H]NMS (12.4 ± 0.2 nM) and graded concentrations of unlabeled carbachol (A), arecoline (B), oxotremorine-M (C), oxotremorine (D), pilocarpine (E), or McN-A-343 (F). The solid line in each panel represents the best fit of eq 3 (n = 1 or 2) to the data from three to seven experiments taken in concert, and the fitted parametric values are listed in Table 5. The sum of squares was significantly lower with two classes of sites than with one ($P \leq 0.0004$) for all ligands except oxotremorine-M, for which one class of sites was sufficient (P = 0.08). The dotted line in each panel depicts the simulated curve for a single class of sites with a value of IC_{50} equal to the value of $IC_{50(L)}$ obtained from the fit of eq 3 (n = 2) to the experimental data. The mean value of $B_{[A]=0}$ for the 27 sets of data represented in the figure was used to obtain the adjusted values of B_{sp} plotted on the y-axes (i.e., 98 ± 11 pM).

dx.doi.org/10.1021/bi4003869 | *Biochemistry* 2013, 52, 7405−7427

Table 6. Affinities of Agonists for the Monomeric and Tetrameric M_2 Receptor in Terms of Schemes 1 and 3

	Scheme 1 (eq 4)[a]				Scheme 3 (eq 6)[b]	
	tetramer		monomer		monomer	
ligand[c]	log K_{A1}	log K_{A2}	log K_{A1}	log K_{A2}	log K_{Ao} or log K_{Aa}	log(αK_{Aa})
oxotremorine-M (8, 3)	−5.76 ± 0.08	−4.52 ± 0.07	−4.05 ± 0.02		−4.06 ± 0.02	−2.29[d]
pilocarpine (5, 4)	−5.54 ± 0.17	−4.43 ± 0.16	−4.43 ± 0.05	−3.25 ± 0.02	−3.90 ± 0.03	−2.86[e]
McN-A-343 (5, 3)	−5.81 ± 0.33	−4.32 ± 0.06	−4.45 ± 0.07	−3.64 ± 0.06	−4.18 ± 0.03	−2.97[e]

[a]The data represented in Figure 5 (reconstituted tetramers) and Figure 12 (monomers) were analyzed in terms of eq 4 (n = 1 or 2) to obtain the fitted values of log K_{Aj} listed here. Single values of log K_{Aj} and F_j were common to the data from all experiments; the value of log K_{Pj} was fixed at −8.45 for tetramers (Table S1 of the Supporting Information) or −8.13 for monomers (see below). The values of F_j were indistinguishable from those obtained with eq 3 (Tables 2 and 5) ($P > 0.07$). [b]The data represented in Figure 12 were analyzed in terms of eq 6. Those obtained with pilocarpine and McN-A-343 were taken in concert as described in Figure S10 and Table S3 of the Supporting Information. The data obtained with oxotremorine-M were analyzed separately, with the value of log K_{Po} taken to be −8.13 (Figure S10 of the Supporting Information). [c]The number of independent experiments is shown in parentheses (tetramer, monomer). [d]The value was taken as that reported previously, and the corresponding value reported for NMS is −2.55.[54] [e]The value was determined as described in the legend of Figure S9 of the Supporting Information.

Binding to Monomers. Purified monomers in solution served as a control for the reconstituted tetramers. Carbachol, arecoline, oxotremorine-M, and oxotremorine bound with Hill coefficients near or indistinguishable from 1 (Table 5), in contrast to the lower values obtained after reconstitution (Table 2). Carbachol, arecoline, and oxotremorine required two classes of sites rather than one in terms of eq 3 ($P \leq 0.0004$); however, the sites of low affinity predominated (i.e., ≥82%), and the area associated with an interconversion from high to low affinity is comparatively small in each case (Figure 12 and Table 5). In assays at graded concentrations of *N*-[^{3}H]methylscopolamine, virtually all of the sites bound the radioligand with an affinity of 6.0 nM [log K_{P1} = −8.22 ± 0.02 (Table S1 of the Supporting Information)]. Detergent-solubilized monomers therefore appeared to be homogeneous or nearly so to those ligands, as expected for a population of mutually independent sites. In contrast, pilocarpine and McN-A-343 revealed a heterogeneity similar to that observed with reconstituted tetramers (cf. Figures 5 and 12 and Tables 2 and 5). To confirm that the system was at equilibrium under the conditions of the assays, the inhibitory effect of pilocarpine was measured after incubation of the reaction mixture for 45 and 180 min. The two sets of data are superimposable (Figure S8 of the Supporting Information), and the observed heterogeneity therefore appears to arise from two or more sites within a monomer.

In accord with the suggestion of a second site, both pilocarpine and McN-A-343 slowed the dissociation of *N*-[^{3}H]-methylscopolamine from the monomeric receptor (Figure S9A,C of the Supporting Information). The effect very likely occurs via the gallamine-specific allosteric site, which has been shown previously to bind *N*-methylscopolamine and oxotremorine-M at sufficiently high concentrations of those ligands.[54] Assays at different concentrations of pilocarpine and McN-A-343 indicated that their affinities for the allosteric site of a receptor bearing *N*-[^{3}H]methylscopolamine at the orthosteric site were 1.4 and 1.1 mM, respectively, as determined from their effect on the rate constant for dissociation of the radioligand (log K_A = −2.86 ± 0.06 and −2.97 ± 0.05; eq S20 of the Supporting Information) (Table 6 and Figure S9D,F of the Supporting Information). In similar experiments with the reconstituted receptor, the affinity of pilocarpine for the allosteric site was 1.7 mM (log K_A = −2.76 ± 0.1) (Figure S9B,E of the Supporting Information).

The inhibitory effects of pilocarpine and McN-A-343 at equilibrium can be described by Scheme 3 (eq 6), in which an unlabeled ligand acts both competitively and noncompetitively via two distinct sites on the monomer (Figure S10 of the Supporting Information). Binding of the unlabeled ligand is determined by four parameters (K_{Ao}, K_{Aa}, α or αK_{Aa}, and β), however, and the data represented in panels E and F of Figure 12 are insufficient to define the system. The number of fitted parameters in eq 6 is reduced by the independent estimate of αK_{Aa} determined kinetically as described above (i.e., αK_{Aa} in Scheme 3 ≡ K_A in eq S20 and Figure S9 of the Supporting Information), but the values of log K_{Ao}, log K_{Aa}, and log β remain highly correlated during successive iterations of the fitting procedure. Because of those correlations and the symmetric nature of the system, which gives rise to equivalent minima in the sum of squares, the data define only one parameter that could be either K_{Ao} or K_{Aa} [i.e., −3.90 ± 0.03 for pilocarpine and −4.18 ± 0.03 for McN-A-343 (Table S3 of the Supporting Information)]. The corresponding values of K_{Aa} or K_{Ao}, respectively, are determined by the value of β.

DISCUSSION

Oligomers and Heterogeneity. The mechanism of GPCR-mediated signaling remains a mystery, but a key lies in the GTP-sensitive dispersion of affinities revealed by agonists. A common view rationalizes those effects in terms of heterogeneity induced by the G protein in an otherwise homogeneous population of mutually independent sites.[3,9,32] Contrary to that view are reports of heterogeneity among purified muscarinic receptors in preparations that lacked or presumably lacked G protein.[27,34−36] Such observations imply that the effect is intrinsic to the receptor alone, but a homogeneous population of independent sites in a system at equilibrium is expected to yield a Hill coefficient of 1, the possibility of interconverting states notwithstanding. This contradiction would be resolved if heterogeneity were to arise from interactions within a homomeric array.

Our results show that M_2 muscarinic receptors purified as monomers and devoid of G protein can appear heterogeneous when reconstituted as oligomers in phospholipid vesicles. Seven agonists and one inverse agonist inhibited the specific binding of *N*-[^{3}H]methylscopolamine with Hill coefficients significantly less than 1. In each case, two classes of sites are required for a description of the data in terms of eq 3. Several lines of evidence attest to the purity of the preparation and suggest that the observed heterogeneity is akin to that displayed by GPCRs in natural tissues.[1−3]

The absence of functionally linked G proteins was confirmed by the failure of GMP-PNP to affect binding of the agonist oxotremorine-M (Figure 4B). *Sf*9 cells express G_i- and G_o-like

proteins that are substrates for pertussis toxin[60] and can be identified in RNA analyses,[61] but their functional interaction with exogenous M_2 receptors or other GPCRs is weak or nonexistent.[60,62−64] They also have not been detected by antibodies to mammalian $G\alpha_{i1-3}$, $G\alpha_o$, or $G\beta$.[60] Any unrecognized association of endogenous G proteins with the M_2 receptor is unlikely to outlast the process of purification and particularly not the final passage on hydroxyapatite, which removes G proteins that otherwise are copurified with the M_2 receptor from myocardial membranes.[27] Silver staining of the purified product from *Sf*9 cells indicated that ∼71% of the protein detected on the gel was intact receptor. Apparent fragments of the receptor were dominated by a 35 kDa species that constituted 11% of the stained protein and may be the first five transmembrane domains. Such a fragment is not expected to bind muscarinic ligands unless it were associated noncovalently with the C-terminal segment, thereby creating a holo-receptor (ref 51 and references cited therein). The balance of 15% consisted of other contaminants. None represented more than ∼2% of the total density, and any contribution to specific binding would be negligible. The purity of the preparation, particularly the absence of G proteins, argues that the observed heterogeneity is a property of the receptor alone.

Purified monomers assembled predominantly or wholly as tetramers upon reconstitution in membranes of POPC, POPS, and cholesterol. The relative molecular mass of the reconstituted complex estimated from its electrophoretic mobility after cross-linking was 5 times that of the monomeric control, a value that is consistent with four protomers after treatment with BS^3. The absence of a band corresponding to a trimer suggests that protomers are not added or removed one at a time and argues for an even number of subunits. Also, the mobility was the same irrespective of whether cross-linking was performed on receptors in vesicles or redissolved in digitonin. The reassembled tetramer therefore is sufficiently stable to survive extraction from the lipid, suggesting that it is not the product of interactions that occur randomly within the vesicle and are trapped by the cross-linker. Essentially the same results were obtained previously when purified monomers of the M_2 receptor were reconstituted in lipids from natural sources.[50]

Receptors were incorporated into phospholipid vesicles at a mean density of 0.3−0.6 protomer per vesicle, as calculated from the vesicular size estimated by dynamic light scattering and the measured quantities of receptor and lipid (Supporting Information). The average number of tetramers per vesicle was therefore 0.08−0.14, leaving at least 86% of the vesicles devoid of receptor. The absence of monomers, dimers, and trimers suggests either that a tetramer was formed before its incorporation or, what seems more likely, that a small fraction of the vesicles took up protomers in sufficient numbers for the emergent tetramers to dominate the signal on Western blots. If fewer than 2% of the vesicles contained all of the receptors (i.e., >30 per vesicle), the number of stranded monomers, dimers, and perhaps trimers would be below the level of detection. The mechanism of such a biased uptake is speculative, although it may be driven by the tendency of receptors to form oligomers. The incorporation of one protomer into a preformed vesicle may favor the incorporation of others, or protomers may exchange between vesicles during a transient phase as the ratio of detergent to lipid is reduced (Supporting Information).

Incorporation of the detergent-solubilized, purified receptor increased the mean hydrodynamic size of the vesicles and the breadth of the distribution (Figure 3). Intensity-based distributions are dominated by larger particles, and the observed changes may represent the emergence of two coexisting populations that make similar contributions to light scattering: a majority of vesicles that have been largely unaffected and a very few that have grown in size because of the selective incorporation of receptor (Supporting Information). Vesicles and other particles smaller than ∼20 nm would not contribute appreciably to the distribution, and their presence therefore cannot be ruled out. They are less likely to occur after extrusion than after sonication, however, and they are unlikely to account for the heterogeneity revealed by agonists. A population of functionally distinct receptors sequestered within a static subpopulation of such vesicles is inconsistent with the effects of *N*-ethylmaleimide and with differences among agonists in the apparent fraction of high-affinity sites (Table 2).

Although the orientation of receptors within the membrane is unknown, none of the sites appears to be sequestered behind a hydrophobic barrier or otherwise inaccessible. The biphasic nature of the inhibition by oxotremorine-M remained the same when incubation was continued beyond 30 min for up to 3 h (Figure S5 of the Supporting Information). Also, the effect of GMP-PNP on the competition between oxotremorine-M and *N*-[^{3}H]methylscopolamine for receptor reconstituted with G proteins is an allosteric interaction that occurs across the membrane (Figure 4A). Finally, *N*-[^{3}H]methylscopamine and the hydrophobic antagonist [^{3}H]quinuclidinylbenzilate labeled the same number of sites (Figure 10). It follows that the vesicles, or at least those containing receptor, were sufficiently leaky for hydrophilic ligands such as *N*-[^{3}H]methylscopolamine, oxotremorine-M, and GMP-PNP to access all reconstituted receptors and G proteins and to equilibrate across the membrane on the time scale of an experiment. Permeability is a non-native condition, and its origin in this case is unclear; nonetheless, it does not appear to compromise effects that, as discussed below, are characteristic of M_2 receptors in their native state.

The orientation of protomers within a tetramer relates in part to their alignment as parallel or antiparallel. The emergence of a single oligomeric state after reconstitution suggests that the formation of tetramers is a specific process, and the functional properties of the reconstituted tetramers differ from those of monomers. These considerations and the recovery of native properties upon reconstitution suggest that the constituent protomers of a tetramer are aligned wholly or predominantly in a parallel manner. Any antiparallel arrangement would be nonphysiological, presumably nonspecific, and unlikely to mimic the properties of native systems.

Heterogeneity and Efficacy. GTP-sensitive heterogeneity in the binding of agonists typically has been detected via the inhibition of a radiolabeled antagonist. Its relevance to signaling was established early on by the observation that the breadth of the dispersion correlates with efficacy.[1−3] Empirical measures of that breadth have included the Hill coefficient (eq 2), the ratio of inhibitory potencies in the presence and absence of a guanylyl nucleotide,[3] and the parameters from a sum of hyperbolic terms (eq 3). In the mechanistically explicit case of the ternary complex model, the breadth is determined by the affinity of the G protein for the receptor in the absence and presence of agonist.[3,30] Measures based on eq 3 or similar expressions have been used most often, and in those cases, efficacy has been shown to correlate with two quantities that reflect the shape of the binding profile: the relative affinity of the agonist for two classes of sites[1,2] and the fraction of labeled sites apparently in the state of higher affinity.[2]

dx.doi.org/10.1021/bi4003869 | *Biochemistry* 2013, 52, 7405−7427

Measures based on the Hill equation tend to be compromised by the nature of the function, which is monophasic and symmetric about the midpoint on semilogarithmic coordinates. The data often are neither, and agreement with the model can be poor. A sum of two or more hyperbolic terms typically provides a good description of the data, but the apparent affinities and the fraction of labeled sites corresponding to one affinity or the other can be highly correlated during successive iterations of the fitting procedure. With the area defined by the relative apparent affinity when n equals 2 (e.g., $\Delta\log IC_{50}$ in eq 3) and the displacement corresponding to the sites of higher affinity (F_H in eq 3), three parameters are reduced to one, and the correlations are avoided (Figure 1 and the Supporting Information).

In native tissues, GTP and analogues such as GMP-PNP promote an apparent interconversion of sites from higher to lower affinity. If the effect is complete and derives strictly from changes in the apparent distribution of sites between states (e.g., F_j in eq 3), as observed with the β-adrenergic receptor,[2] the product $F_H\ \Delta\log IC_{50}$ is a quantitative measure not only of the dispersion but also of the shift effected by GTP. With receptor devoid of G protein, the product $F_H\ \Delta\log IC_{50}$ represents the potential for a GTP-induced shift if such an effect were possible. It therefore has been used to compare the heterogeneity revealed by agonists at the reconstituted M_2 receptor with properties of the receptor in native membranes. The characteristic effect of GMP-PNP was observed when the purified M_2 receptor was reconstituted with G proteins (Figure 4A), confirming that the system is capable of a typical response when both components are present.

As used here, the area represented by $F_H\ \Delta\log IC_{50}$ is a descriptor of behavior in the absence of G proteins and guanylyl nucleotide. Cardiac muscarinic receptors and some other GPCRs can exhibit three classes of sites under some conditions (e.g., ref 49 and references cited therein), and the effect of a guanylyl nucleotide can diverge from the general pattern described above. Although the preexisting sites of lowest affinity typically are indistinguishable from those induced by GMP-PNP (e.g., ref 49), induced sites of even lower affinity have been observed in some cases.[65] Such behavior suggests that heterogeneity intrinsic to the receptor can be modulated by the G protein. The effect of GMP-PNP also can be incomplete, with sites of higher affinity persisting at saturating concentrations of the nucleotide (e.g., Figure 4A and ref 31). In addition, some receptors may be sequestered in a compartment devoid of G protein.[7,31] Predictions based on $F_H\ \Delta\log IC_{50}$ measured with the receptor alone therefore must be qualified accordingly when considering behavior in the presence of G proteins and guanylyl nucleotides.

The potential shifts estimated for seven agonists and two of the three antagonists are compared with measures of efficacy in Figure 13A. The latter were calculated from intrinsic activities reported for regulation of the M_2 receptor by the same ligands in biochemical assays, as described in the legend of Figure 13 and summarized in Table S4 of the Supporting Information. Activities mediated by different G proteins were pooled on the assumption that the reconstituted receptor could form a productive complex with any particular G protein. Ligands with broader binding profiles tend to be more efficacious [$P < 0.00001$ (Figure 13A and Table S4A of the Supporting Information)], as described previously for GPCRs in natural membranes.[1−3] The breadth of the dispersion displayed by reconstituted tetramers also tracks that reported for binding to M_2 receptors in natural membranes, as quantified by the potential shift [$P = 0.00002$ (Figure 13B and Table S4A of the Supporting Information)] and the Hill coefficient [$P < 0.00001$ (Figure 13C and Table S4A of the Supporting Information)]. These comparisons suggest that the heterogeneity found after reconstitution without G proteins is a determinant of efficacy (Figure 13A) and similar in kind to the heterogeneity displayed

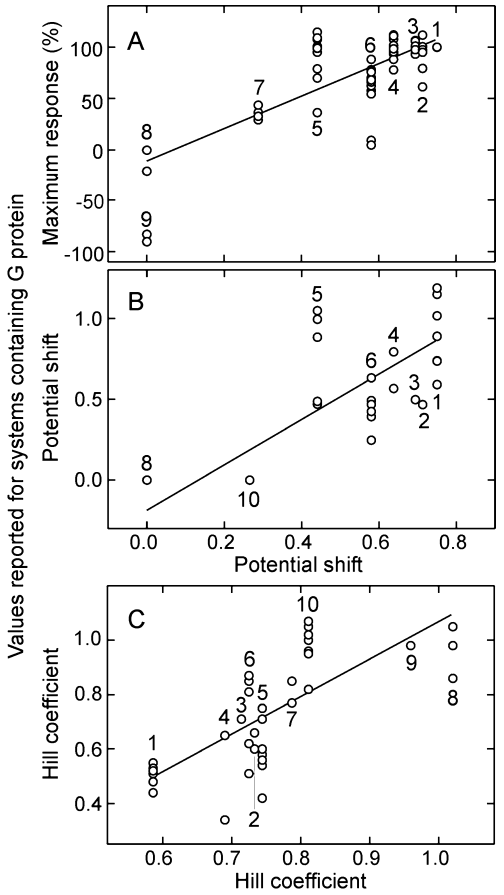

Figure 13. Comparison of heterogeneity and response among ligands at the M_2 muscarinic receptor in reconstituted preparations and native membranes. The numbering of ligands corresponds to that in Table 2 and Table S4 of the Supporting Information: 1, carbachol; 2, arecoline; 3, bethanechol; 4, oxotremorine-M; 5, oxotremorine; 6, pilocarpine; 7, McN-A-343; 8, quinuclidinylbenzilate; 9, *N*-methylscopolamine; 10, atropine. (A) The potential shifts listed in Table 2 are compared with the intrinsic activities reported previously for the inhibition of adenylate cyclase, hydrolysis of GTP, binding of [^{35}S]GTPγS, stimulation of phospholipase C, or stimulation of adenylate cyclase in preparations pretreated with pertussis toxin. Intrinsic activity was taken as the maximal response to a particular ligand expressed as a percentage of the maximal response to carbachol or methacholine in the same investigation. The potential shift for atropine is excluded from the comparison in panel A, as described in the text. (B) The potential shifts listed in Table 2 are compared with the potential shifts calculated from the parametric values reported previously for analyses of binding profiles in terms of eq 3 or equivalent expressions. (C) The Hill coefficients listed in Table 2 are compared with values of n_H reported previously. In each panel, the values from Table 2 are plotted on the *x*-axis. Values plotted on the *y*-axis are the individual values from each report; the values (A) and means (A−C) are listed in Table S4 of the Supporting Information, and further details are described in the accompanying footnotes. The lines were obtained by linear regression, and the correlation is significant in each case ($P \leq 0.00002$). The fitted parametric values are as follows: (A) slope of 157 ± 17 and *y*-intercept of -10 ± 10, (B) slope of 1.41 ± 0.27 and *y*-intercept of -0.19 ± 0.16, and (C) slope of 1.38 ± 0.20 and *y*-intercept of -0.31 ± 0.15.

dx.doi.org/10.1021/bi4003869 | *Biochemistry* 2013, 52, 7405−7427

by M_2 receptors in G protein-containing preparations such as myocardial membranes (Figure 13B,C).

The relationship among agonists between high-affinity binding and efficacy cannot be extended to atropine, which is an inverse agonist[19,22] and therefore must discern heterogeneity in a different way. Such a difference is detected in the effect of guanylyl nucleotides on cardiac muscarinic receptors, where the apparent interconversion from high to low affinity for agonists is mirrored by a concomitant interconversion from low to high affinity for some antagonists.[31,50,56,66] It follows that the predictor of efficacy in the case of an inverse agonist such as atropine may be the low-affinity component of the binding profile.

Although the sensitivity to a guanylyl nucleotide cannot be tested in the absence of a G protein, a similar but opposite effect is obtained upon alkylation of the receptor with *N*-ethylmaleimide. Treatment with *N*-ethylmaleimide has been shown to increase the overall affinity of the M_2 receptor for agonists,[55,56] while that for antagonists is either unchanged or reduced.[48,55,56] The effect can be described empirically as an interconversion from one state of affinity to another, with the reagent favoring agonist-preferred, active states over antagonist-preferred, inactive states.[48,67] It occurs in the absence of G proteins and therefore has been used here to distinguish between the heterogeneity revealed by agonists and antagonists.

Reconstituted M_2 receptors mimicked their counterparts in natural membranes, in that alkylation increased their overall affinity for oxotremorine-M and decreased that for *N*-[^{3}H]-methylscopolamine and atropine. In terms of Scheme 1, there was an apparent redistribution of sites from states of lower affinity for the agonist and higher affinity for antagonists to states of higher affinity for the agonist and lower affinity for antagonists. There was little or no change in the oligomeric status of the purified receptor before or after reconstitution, as monitored by electrophoretic mobility after cross-linking. This differential effect of *N*-ethylmaleimide reinforces the link between heterogeneity and efficacy that emerges from the comparison in Figure 13A. Alkylation also reduced the capacity for *N*-[^{3}H]methylscopolamine to 60% of that of an untreated control. Such a loss has been observed previously and attributed to alkylation-induced instability, in accord with the notion that the reagent promotes an active and comparatively unstable state of GPCRs.[48]

The quantity described here as the potential shift facilitates a comparison of binding and efficacy, but the values of the constituent parameters are masked. Of the full agonists listed in Table 2, arecoline and bethanechol gave values of F_H near 0.2 and differed in their apparent affinity for the two states of the receptor by more than 2000-fold [$IC_{50(L)}/IC_{50(H)}$]. The corresponding binding profiles are visually distinct, as illustrated in panels B and C of Figure 5. In contrast, carbachol and oxotremorine-M gave values of F_H near 0.5 and a difference of ~30-fold in their apparent affinity for the two states. There accordingly is an inverse relationship between the ratio of affinities and the apparent fraction of sites in the state of high affinity, at least among those four agonists. Similar trends have been observed previously, and the correlation can be positive or negative (e.g., refs 2, 30, and 58). Although the mechanistic basis of such relationships only can be surmised in the case of an empirical expression such as eq 3, interactions between the protomers of an oligomer offer a plausible model in the context of a reconstituted tetramer.[58]

In contrast to reconstituted tetramers, purified monomers in solution appeared to be homogeneous or nearly so to most agonists (Figure 12 and Table 5). With the exception of pilocarpine and McN-A-343, discussed below, the Hill coefficients were near or indistinguishable from 1, and the potential shifts calculated from the fitted parameters of eq 3 were comparatively small. The latter derive from a minor fraction of high-affinity sites [≤18% (Table 5)], which may represent the small population of dimers and tetramers identified after cross-linking [21% (Table 1)]. The potential shifts are not correlated with intrinsic activity (Figure S11A of the Supporting Information), nor are the potential shifts or the Hill coefficients correlated with the corresponding parameters in other reports (Figure S11B,C of the Supporting Information).

Oligomeric status is a major but not the sole determinant of differences between monomers in solution and tetramers in vesicles. Other factors include the difference in the environment between phospholipid vesicles on one hand and detergent micelles on the other, which affects the affinity of muscarinic ligands and may have other consequences. To confirm that the homogeneous behavior of monomers in the binding assays is a property of the monomeric state, purified monomers were reconstituted in nanodisks of POPC and membrane scaffold protein in the manner described previously.[68] The Hill coefficient was indistinguishable from 1 for *N*-[^{3}H]-methylscopolamine ($\log EC_{50} = -8.64 \pm 0.07$, eq 1, $N = 3$) and for its inhibition by oxotremorine-M ($\log IC_{50} = -3.96 \pm 0.08$, eq 2, $N = 3$).[c]

The decrease in n_H and the increase in potential shift that accompany reconstitution of the purified receptor (cf. Tables 2 and 5) are consistent with the notion that an essentially homogeneous population of sites becomes heterogeneous when mutually independent monomers are reassembled as tetramers. They indicate that the heterogeneity revealed by agonists at GPCRs is a property of the receptor alone in its oligomeric state, arising from constitutive asymmetry or cooperativity in the binding of the ligand. The heterogeneity is not induced by G proteins, although it may be modulated by them.

Allosteric Site. In the case of pilocarpine and McN-A-343, the values of n_H and the potential shift obtained with monomers were similar to the corresponding values after reconstitution (cf. Tables 2 and 5). Heterogeneity is unexpected for binding to the single orthosteric site of a monomer in a system at equilibrium, and the presence of a second, allosteric site was confirmed by the decrease effected by both ligands in the rate of dissociation of *N*-[^{3}H]methylscopolamine (Figure S9 of the Supporting Information). The same effect has been observed previously with oxotremorine-M and *N*-methylscopolamine, which were shown to act via the allosteric site recognized by gallamine.[54] These observations suggest that the heterogeneity revealed by pilocarpine and McN-A-343 at purified monomers is the net result of competitive inhibition at the orthosteric site and noncompetitive effects via the allosteric site.

The dual effect of pilocarpine and McN-A-343 at purified monomers is depicted in Scheme 3, in which the ligand may bind to the orthosteric site (K_{Ao}) or the allosteric site (K_{Aa}) of an otherwise vacant receptor. Only one such affinity is defined by the data represented in Figure 12, and it could be either K_{Ao} or K_{Aa} (Figure S10 and Table S3 of the Supporting Information). The corresponding value of K_{Aa} or K_{Ao} is larger by a factor that depends upon the values of α and β, neither of which is defined explicitly by the present data. The smaller, defined value of $K_{Aa/o}$ is listed in Table 6 together with the affinity of the agonist for the

dx.doi.org/10.1021/bi4003869 | *Biochemistry* 2013, 52, 7405−7427

NMS-occupied receptor (αK_{Aa}), which was determined from its effect on the rate of dissociation of *N*-[^{3}H]methylscopolamine and taken to be a constant in Scheme 3. Although the larger value of $K_{Aa/o}$ is undefined, it can be shown to exceed the value of αK_{Aa} for both agonists.

The smaller of the two values derived from Scheme 3 appears to be the affinity for the orthosteric site, at least in the case of pilocarpine. Tyrosine 403 participates in the binding of quinuclidinylbenzilate to the orthosteric site of the M_2 receptor,[69] and its mutation to phenylalanine or alanine reduced the affinity of pilocarpine by 38−90-fold.[70,71] In contrast, mutations at the allosteric site were essentially without effect.[71] The inhibitory effect in those studies therefore was dominated by the interaction at the orthosteric site, and the rank order affinities therefore is as follows: $K_{Ao} < \alpha K_{Aa} < K_{Aa}$. That in turn implies that the allosteric interaction between *N*-[^{3}H]methylscopolamine and the agonist is positively cooperative with pilocarpine and perhaps with McN-A-343 [i.e., $\alpha < 1$ (Table S3 of the Supporting Information)]. Consistent with this conclusion, the level of binding of *N*-[^{3}H]methylscopolamine to the M_2 receptor was increased by a truncated derivative of McN-A-343 that bound only to the allosteric site.[72]

Also listed in Table 6 are the affinities estimated for monomers and reconstituted tetramers in terms of Scheme 1, in which all binding is to the orthosteric site and therefore strictly competitive. Schemes 1 and 3 yield similar estimates for the affinities of pilocarpine and McN-A-343 at purified monomers (Table 6), in accord with the notion of dual competitive and noncompetitive effects. The affinities for reconstituted tetramers in terms of Scheme 1 are somewhat higher than those for monomers, but there is a degree of overlap that can be seen when the data and fitted curves from Figures 5 and 12 are superimposed for each ligand (Figure S12 of the Supporting Information). McN-A-343 is only 2.5-fold more potent overall at tetramers, and pilocarpine is 16-fold more potent (Table S5 of the Supporting Information). This comparison suggests that there also is an allosteric contribution to the inhibitory effect of those agonists at tetramers. If so, the orthosteric contribution is overstated by the potential shifts listed in Table 2. That in turn may account for the observation that the shift for pilocarpine, which is a partial agonist in most systems, exceeds that for the full agonist oxotremorine (Table 2 and Figure 13A).

Whereas the dual effect of pilocarpine and McN-A-343 at monomers is evident in the multiphasic inhibitory behavior of each ligand, oxotremorine-M exhibited a Hill coefficient indistinguishable from 1 and therefore appears to act at a single site. A similar analysis in terms of Scheme 3 yields a value of $10^{-4.06}$ M for K_{Ao} or K_{Aa} (Table 6), which agrees closely with the value of K_{A1} obtained for competitive inhibition in terms of Scheme 1. Also, the replacement of tyrosine with phenylalanine at position 403 of the M_2 receptor reduced its affinity for oxotremorine-M by ∼40-fold,[70] consistent with binding to the orthosteric site. It follows that the affinity returned by Scheme 3 is K_{Ao} and that the inhibitory effect of oxotremorine-M at monomers is likely to be wholly competitive.

Among the full agonists carbachol, arecoline, oxotremorine-M, and oxotremorine, the difference in overall potency at monomers and tetramers ranged from 16-fold with oxotremorine-M to 50-fold with carbachol (Figure S12 and Table S5 of the Supporting Information). With carbachol, arecoline, and oxotremorine, the binding to tetramers was inhibited by ∼80% at concentrations that caused 20% inhibition in monomers. Also, pilocarpine has been tested for its slowing effect on the dissociation of *N*-[^{3}H]methylscopolamine from monomers and tetramers, and its affinity for the allosteric site of the radioligand-occupied receptor is the same in both preparations [log $\alpha K_{Aa} > 1$ mM (Figure S9 of the Supporting Information)]. If the full agonists are similarly weak at the allosteric site, it seems likely that the heterogeneity and potential shift measured after reconstitution derived largely or wholly from interactions at orthosteric sites.

Although the foregoing considerations suggest that full agonists are orthosteric in their effect on the binding of *N*-[^{3}H]methylscopolamine to tetramers, an allosteric component cannot be ruled out. The oligomeric nature of M_2 muscarinic receptors in preparations from heart and *Sf*9 cells can be inferred from the dose-dependent effects of gallamine on the binding of orthosteric ligands, and its affinity for constituent protomers can differ by as much as 200-fold.[73] Such differences indicate that the consequences of interactions among eight orthosteric and allosteric sites are not readily predictable. Also, it has been suggested that interactions within the allosteric vestibule of the M_2 receptor are involved in conformational changes linked to the activation of G_s and G_i.[74] If the allosteric site turns out to be a determinant of heterogeneity in reconstituted tetramers of the M_2 receptor, the binding properties of purified monomers suggest that its contribution is itself a product of the tetrameric state. Moreover, the generality of GTP-sensitive heterogeneity raises the possibility of a counterpart in other GPCRs.

Oligomers, Cooperativity, and Signaling. In light of the relationship between the binding properties of reconstituted tetramers and efficacy, the mechanistic basis of heterogeneity in those preparations has implications for the mechanism of signaling. If the system is at thermodynamic equilibrium, heterogeneity within an oligomer is indicative of constitutive asymmetry, cooperativity, or both. It has been shown previously that the multiphasic binding of agonists to the cardiac muscarinic receptor can be described quantitatively by a scheme in which a tetravalent receptor interconverts spontaneously between two states differing in their cooperative properties and perhaps in their asymmetry.[27,45,49,50] Such agreement raises the possibility that interactions within the oligomer are an intrinsic part of the signaling process.

Asymmetry alone cannot account for the binding properties of the reconstituted tetramer. Such a model failed to yield consistent values for the affinity of *N*-[^{3}H]methylscopolamine as measured with the radioligand alone and as inferred from its effect on the inhibitory potency of unlabeled ligands (Figure 9). A cooperative component therefore appears to be present, and cooperativity alone is sufficient to describe the data. A blend of asymmetry and cooperativity also is a possibility, however, because of the ambiguity of the data when both are present. If the specific signal from the probe is invariant, as in the case of a radioligand, every asymmetric solution has a symmetric equivalent.

In previous studies of the M_2 receptor in detergent-solubilized,[59] purified,[27] and reconstituted preparations,[50] cooperative effects have emerged from a difference in the apparent capacity for *N*-[^{3}H]methylscopolamine and [^{3}H]-quinuclidinylbenzilate. Such a difference taken alone can be rationalized as cooperativity or asymmetry,[57] but the cooperative nature of the system was evident in the inhibition of [^{3}H]quinuclidinylbenzilate by unlabeled *N*-methylscopolamine at sites that were inaccessible to the radiolabeled form of the latter. The same comparison is not possible with the reconstituted tetramers described here, which exhibit the same capacity for both radioligands.

Other examples of GPCRs that have been reported to exhibit cooperativity in the binding of ligands at thermodynamic equilibrium include the D_2 dopamine receptor,[75] the D_1 dopamine and adenosine receptors,[76] the histamine receptor,[58] and the opiate receptor.[37] Evidence from kinetic studies has argued for cooperative effects at the glycoprotein hormone receptor,[77] the vasopressin and oxytocin receptors,[78] and the D_2 dopamine receptor.[79] More recently, FRET between fluorophore-tagged protomers has been used to identify cooperativity in live cells expressing the vasopressin, oxytocin, and D_2 dopamine receptors.[80] A molecular dynamics simulation of a dimer of rhodopsin has suggested that light activation of one protomer opens a hydrophobic cleft in the contiguous protomer, which in turn facilitates the interaction of the latter with transducin.[81] In studies of functional complementation within homo- or heterodimers of Family 1 and 3 GPCRs, one protomer has been shown to regulate the activation of another.[82,83] Asymmetry within an oligomer of receptors may be constitutive, or it may be introduced by another party such as a G protein. A dimer of the leukotriene B_4 receptor has been copurified with 1 equiv of $G\alpha_{i2}$,[84] and molecular modeling has suggested that the ratio of rhodopsin to transducin is 2:1.[85]

Several lines of evidence now suggest that M_2 muscarinic receptors exist wholly or largely as tetramers in various preparations. Monomers purified from *Sf*9 cells have been shown to assemble spontaneously as tetramers when reconstituted with lipids purified from bovine brain.[50] A complex containing three, differently tagged variants of the M_2 receptor has been purified from triply infected *Sf*9 cells in quantities sufficient to suggest a species larger than a trimer,[41] and measurements of the FRET efficiency between fluorophore-tagged protomers have suggested that M_2 receptors form tetramers in transfected CHO cells.[42] At least four interacting sites are required if cooperative interactions are to account for the GMP-PNP-sensitive binding of agonists to M_2 muscarinic receptors in myocardial membranes and in a purified complex with G proteins.[27,49] Similarly, four sites are required to account for noncompetitive effects in the binding of antagonists[27,50,59] and for the allosteric effects of gallamine on the binding of *N*-[^{3}H]methylscopolamine.[73] With other GPCRs, measurements of FRET coupled with bimolecular complementation or sequential energy transfer have identified oligomers that are at least trimers (e.g., refs 86 and 87) or tetramers (e.g., ref 88).

The observations recounted above suggest that oligomers and cooperativity are common features of GPCRs, but monomers tend to be invisible or detected only by inference in such approaches. In contrast, techniques based on measurements of single particles have identified monomers as well as oligomers of various sizes. Some studies based on total internal reflection fluorescence microscopy have suggested that the receptors are predominantly monomeric with a minor contingent of dimers (e.g., ref 89), while others have identified dimers and larger oligomers of different sizes up to octamers (e.g., ref 90). Higher-order intensity studies such as fluorescence correlation spectroscopy and number and brightness analysis have revealed a prevalence of dimers or heterotetramers in some cases,[91,92] and the clustering of receptors in multiprotein nanodomains in another.[93] The reasons for such disparate results are not clear, although the failure of agonists to perturb the apparent distribution of protomers among different states of aggregation,[89−92] at least in the case of homooligomers, suggests that the oligomeric status of receptors tracked in those studies is not a determinant of signaling.

Uncertainty over the prevalence and stability of oligomers extends to their functional role. They appear to be required for trafficking of the receptor to the plasma membrane, at least for some GPCRs,[94] and hetero-oligomerization appears to create new signaling entities with distinct pharmacologies (reviewed in refs 37 and 95). A role for oligomers in the propagation of a signal is suggested by evidence that a ligand acting at one protomer can elicit a functional response at another (e.g., refs 81−83). Finally, GPCRs are known to adopt multiple states that differ in their functionality. The capacity of a ligand to favor one state of a system over another depends upon the difference in its affinity for the two states. An oligomer with two or more sites is an integrator that sums the free energies of all microscopic processes that can occur within the complex, yielding the net affinity for a particular state at a particular concentration of the ligand. In such a system, the distribution of receptors among different states can have a range of sensitivities to concentration-dependent modulation; in contrast, the concentration dependence in a system with only one site will be strictly rectangular hyperbolic. This potential for control is extended in GPCRs by the allosteric interaction between agonists and guanylyl nucleotides. The identification of efficacy-linked heterogeneity in reconstituted tetramers of the M_2 receptor suggests that oligomers are the basic unit of signaling. A heteromeric complex comprising four interacting protomers of receptor linked to two or more interacting G proteins would be a system of formidable complexity and offer impressive potential for ligand-based control.

Doubt about the role of oligomers in GPCR-mediated signaling derives in part from the properties of monomers reconstituted in nanodisks, where they activate G proteins and exhibit guanylyl nucleotide-sensitive heterogeneity in the binding of agonists.[18,96−98] In those preparations, however, the binding profiles were biphasic only at subsaturating concentrations of G protein; that is, the fraction of sites exhibiting a higher affinity increased from zero with the receptor alone to 100% when the G protein was present at saturating concentrations.[98] Heterogeneity therefore was induced by the G protein, in contrast to what has been observed with G protein-free tetramers. Moreover, the notion that heterogeneity requires an excess of receptors over G proteins is at variance with reports that the binding of agonists to muscarinic receptors can be biphasic in reconstituted preparations when G proteins are saturating or likely to be saturating,[35,50] even when the receptors and G proteins are of one subtype.[47] It also is difficult to reconcile with reports that the fraction of sites in one state or the other varies from agonist to agonist under conditions when the ratio of G proteins to receptors is expected to be constant (e.g., refs 1, 2, 58, and 99). These considerations suggest that the heterogeneity displayed by monomers reconstituted with G proteins is different in kind from that of reconstituted tetramers or receptors in natural membranes.

■ ASSOCIATED CONTENT

Ⓢ Supporting Information

Calculation of the area representing the potential effect of a guanylyl nucleotide on the binding of an agonist (pp S-1−S-3, eqs S1−S17), estimation of the number of M_2 receptors reconstituted per vesicle (pp S-3−S-4, eq S18), effect of detergent on vesicular size (Figure S1), detection of oligomers by co-immunoprecipitation of differently tagged protomers (Figure S2), concentration dependence of cross-linking by BS^3 (Figure S3), homogeneity of the purified M_2 receptor

determined by silver staining and immunoblotting (Figure S4), binding parameters of [^{3}H]NMS in all preparations of the M_2 receptor (Table S1), equilibration of carbachol with reconstituted tetramers of the M_2 receptor (Figure S5), effect of *N*-ethylmaleimide on binding to reconstituted tetramers modeled as two classes of sites (Figure S6 and Table S2), binding of agonists to reconstituted tetramers modeled as four interacting sites (Figure S7), equilibration of pilocarpine with purified monomers of the M_2 receptor (Figure S8), allosteric effects of pilocarpine and McN-A-343 on the binding of [^{3}H]NMS in assays under kinetic and thermodynamic control (Figures S9 and S10, eq S20, and Table S3), sources and description of the published data plotted in Figures 13 and S8 (Table S4), comparison of binding and response between monomers and M_2 receptors in native membranes (Figure S11), and comparison of binding to monomers and reconstituted tetramers (Figure S12). This material is available free of charge via the Internet at http://pubs.acs.org.

AUTHOR INFORMATION

Corresponding Author

*Leslie Dan Faculty of Pharmacy, University of Toronto, 144 College St., Toronto, Ontario, Canada M5S 3M2. E-mail: jwells@phm.utoronto.ca. Phone: (416) 978-3068. Fax: (416) 978-8511.

Funding

This work was supported by grants from the Canadian Institutes of Health Research (Grant MOP 97978 to J.W.W.), the Heart and Stroke Foundation of Ontario (Grants T6280 and NA 7168 to J.W.W.), and the Natural Sciences and Engineering Research Council of Canada (Grant 341920-2010 to H.H.). D.S.R. was the recipient of a scholarship from the Natural Sciences and Engineering Research Council of Canada and an Ontario Graduate Scholarship.

Notes

The authors declare no competing financial interest.

ACKNOWLEDGMENTS

We are grateful to Hiren Patel for assistance with measurements of light scattering, to Helen Fan for conducting the phosphate assay, and to Rabindra V. Shivnaraine for helpful discussions over the course of the investigation.

ABBREVIATIONS

ABT, 3-(2′-aminobenzhydryloxy)tropane; BS^3, bis-(sulfosuccinimidyl)suberate; DEAE, diethylaminoethyl; EDTA, ethylenediaminetetraacetic acid; FRET, Förster resonance energy transfer; Gα and Gβ, α- and β-subunits of G proteins, respectively; GMP-PNP, guanylylimidodiphosphate; GPCR, G protein-coupled receptor; HA, influenza hemagglutin; HEPES, sodium *N*-(2-hydroxyethyl)piperazine-*N*′-2-ethanesulfonate; IB, immunoblot; IP, immunoprecipitation; M_2R, M_2 muscarinic acetylcholine receptor; NEM, *N*-ethylmaleimide; NMS, *N*-methylscopolamine; PMSF, phenylmethanesulfonyl fluoride; POPC, 1-pamitoyl-2-oleoyl-*sn*-glycero-3-phosphocholine; POPS, 1-pamitoyl-2-oleoyl-*sn*-glycero-3-phospho-L-serine; QNB, quinuclidinylbenzilate; SEM, standard error of the mean; *Sf*9, *Spodoptera frugiperda*; Tris, tris(hydroxymethyl)-aminomethane.

ADDITIONAL NOTES

[a]GPCRs interconvert spontaneously between at least two states, an active state and an inactive state. As used here, the term "antagonist" includes ligands that bind to both states with the same affinity (i.e., classical antagonists) and those that bind preferentially to the inactive state (i.e., inverse agonists). The distinction is not readily apparent when the ligand-free system is wholly or predominantly in the inactive state.

[b]The partition coefficients are available in the PubChem Substance and Compound database through the unique chemical structure identifiers CID: 656633 (NMS) and CID: 23056 (QNB) (http://pubchem.ncbi.nlm.nih.gov).

[c]D. S. Redka, T. Morizumi, P. Paranthaman, O. P. Ernst, and J. W. Wells, unpublished observations.

REFERENCES

(1) Birdsall, N. J., Burgen, A. S., and Hulme, E. C. (1978) The binding of agonists to brain muscarinic receptors. *Mol. Pharmacol. 14*, 723−736.

(2) Kent, R. S., De Lean, A., and Lefkowitz, R. J. (1980) A quantitative analysis of β-adrenergic receptor interactions: Resolution of high and low affinity states of the receptor by computer modeling of ligand binding data. *Mol. Pharmacol. 17*, 14−23.

(3) Ehlert, F. J. (1985) The relationship between muscarinic receptor occupancy and adenylate cyclase inhibition in the rabbit myocardium. *Mol. Pharmacol. 28*, 410−421.

(4) Berrie, C. P., Birdsall, N. J., Burgen, A. S., and Hulme, E. C. (1979) Guanine nucleotides modulate muscarinic receptor binding in the heart. *Biochem. Biophys. Res. Commun. 87*, 1000−1005.

(5) Sibley, D. R., and Creese, I. (1983) Interactions of ergot alkaloids with anterior pituitary D-2 dopamine receptors. *Mol. Pharmacol. 23*, 585−593.

(6) Battaglia, G., Shannon, M., and Titeler, M. (1984) Guanyl nucleotide and divalent cation regulation of cortical S_2 serotonin receptors. *J. Neurochem. 43*, 1213−1219.

(7) Neubig, R. R., Gantzos, R. D., and Brasier, R. S. (1985) Agonist and antagonist binding to α_2-adrenergic receptors in purified membranes from human platelets. Implications of receptor-inhibitory nucleotide-binding protein stoichiometry. *Mol. Pharmacol. 28*, 475−486.

(8) Ross, E. M., Maguire, M. E., Sturgill, T. W., Biltonen, R. L., and Gilman, A. G. (1977) Relationship between the β-adrenergic receptor and adenylate cyclase. *J. Biol. Chem. 252*, 5761−5775.

(9) De Lean, A., Stadel, J. M., and Lefkowitz, R. J. (1980) A ternary complex model explains the agonist-specific binding properties of the adenylate cyclase-coupled β-adrenergic receptor. *J. Biol. Chem. 255*, 7108−7117.

(10) Bornancin, F., Pfister, C., and Chabre, M. (1989) The transitory complex between photoexcited rhodopsin and transducin. Reciprocal interaction between the retinal site in rhodopsin and the nucleotide site in transducin. *Eur. J. Biochem. 184*, 687−698.

(11) Onaran, H. O., Costa, T., and Rodbard, D. (1993) $\beta\gamma$ subunits of guanine nucleotide-binding proteins and regulation of spontaneous receptor activity: Thermodynamic model for the interaction between receptors and guanine nucleotide-binding protein subunits. *Mol. Pharmacol. 43*, 245−256.

(12) Conklin, B. R., and Bourne, H. R. (1993) Structural elements of Gα subunits that interact with G$\beta\gamma$, receptors, and effectors. *Cell 73*, 631−641.

(13) Birnbaumer, L., Abramowitz, J., and Brown, A. M. (1990) Receptor-effector coupling by G proteins. *Biochim. Biophys. Acta 1031*, 163−224.

(14) Hargrave, P. A., Hamm, H. E., and Hofmann, K. P. (1993) Interaction of rhodopsin with the G-protein, transducin. *BioEssays 15*, 43−50.

(15) Limbird, L. E., and Lefkowitz, R. J. (1978) Agonist-induced increase in apparent β-adrenergic receptor size. *Proc. Natl. Acad. Sci. U.S.A. 75*, 228−232.

(16) Matesic, D. F., Manning, D. R., and Luthin, G. R. (1991) Tissue-dependent association of muscarinic acetylcholine receptors with guanine nucleotide-binding regulatory proteins. *Mol. Pharmacol. 40*, 347−353.
(17) Kuravi, S., Lan, T. H., Barik, A., and Lambert, N. A. (2010) Third-party bioluminescence resonance energy transfer indicates constitutive association of membrane proteins: Application to class a G-protein-coupled receptors and G-proteins. *Biophys. J. 98*, 2391−2399.
(18) Yao, X. J., Velez, Ruiz, G., Whorton, M. R., Rasmussen, S. G., Devree, B. T., Deupi, X., Sunahara, R. K., and Kobilka, B. (2009) The effect of ligand efficacy on the formation and stability of a GPCR-G protein complex. *Proc. Natl. Acad. Sci. U.S.A. 106*, 9501−9506.
(19) Jakubik, J., Bacakova, L., el-Fakahany, E. E., and Tucek, S. (1995) Constitutive activity of the M_1−M_4 subtypes of muscarinic receptors in transfected CHO cells and of muscarinic receptors in the heart cells revealed by negative antagonists. *FEBS Lett. 377*, 275−279.
(20) Seifert, R., and Wenzel-Seifert, K. (2002) Constitutive activity of G-protein-coupled receptors: Cause of disease and common property of wild-type receptors. *Naunyn-Schmiedeberg's Arch. Pharmacol. 366*, 381−416.
(21) Ren, Q., Kurose, H., Lefkowitz, R. J., and Cotecchia, S. (1993) Constitutively active mutants of the α_2-adrenergic receptor. *J. Biol. Chem. 268*, 16483−16487.
(22) Spalding, T. A., Burstein, E. S., Wells, J. W., and Brann, M. R. (1997) Constitutive activation of the m5 muscarinic receptor by a series of mutations at the extracellular end of transmembrane 6. *Biochemistry 36*, 10109−10116.
(23) Rasmussen, S. G., Jensen, A. D., Liapakis, G., Ghanouni, P., Javitch, J. A., and Gether, U. (1999) Mutation of a highly conserved aspartic acid in the β_2 adrenergic receptor: Constitutive activation, structural instability, and conformational rearrangement of transmembrane segment 6. *Mol. Pharmacol. 56*, 175−184.
(24) Burstein, E. S., Spalding, T. A., and Brann, M. R. (1997) Pharmacology of muscarinic receptor subtypes constitutively activated by G proteins. *Mol. Pharmacol. 51*, 312−319.
(25) Bunemann, M., Frank, M., and Lohse, M. J. (2003) G_i protein activation in intact cells involves subunit rearrangement rather than dissociation. *Proc. Natl. Acad. Sci. U.S.A. 100*, 16077−16082.
(26) Gales, C., Van Durm, J. J., Schaak, S., Pontier, S., Percherancier, Y., Audet, M., Paris, H., and Bouvier, M. (2006) Probing the activation-promoted structural rearrangements in preassembled receptor-G protein complexes. *Nat. Struct. Mol. Biol. 13*, 778−786.
(27) Wreggett, K. A., and Wells, J. W. (1995) Cooperativity manifest in the binding properties of purified cardiac muscarinic receptors. *J. Biol. Chem. 270*, 22488−22499.
(28) Ma, A. W.-S., Pawagi, A. B., and Wells, J. W. (2008) Heterooligomers of the muscarinic receptor and G proteins purified from porcine atria. *Biochem. Biophys. Res. Commun. 374*, 128−133.
(29) Dupre, D. J., Robitaille, M., Ethier, N., Villeneuve, L. R., Mamarbachi, A. M., and Hebert, T. E. (2006) Seven transmembrane receptor core signaling complexes are assembled prior to plasma membrane trafficking. *J. Biol. Chem. 281*, 34561−34573.
(30) Lee, T. W., Sole, M. J., and Wells, J. W. (1986) Assessment of a ternary model for the binding of agonists to neurohumoral receptors. *Biochemistry 25*, 7009−7020.
(31) Green, M. A., Chidiac, P., and Wells, J. W. (1997) Cardiac muscarinic receptors. Relationship between the G protein and multiple states of affinity. *Biochemistry 36*, 7380−7394.
(32) Minton, A. P., and Sokolovsky, M. (1990) A model for the interaction of muscarinic receptors, agonists, and two distinct effector substances. *Biochemistry 29*, 1586−1593.
(33) Sternweis, P. C., and Robishaw, J. D. (1984) Isolation of two proteins with high affinity for guanine nucleotides from membranes of bovine brain. *J. Biol. Chem. 259*, 13806−13813.
(34) Peterson, G. L., Herron, G. S., Yamaki, M., Fullerton, D. S., and Schimerlik, M. I. (1984) Purification of the muscarinic acetylcholine receptor from porcine atria. *Proc. Natl. Acad. Sci. U.S.A. 81*, 4993−4997.
(35) Haga, K., Haga, T., and Ichiyama, A. (1986) Reconstitution of the muscarinic acetylcholine receptor. Guanine nucleotide-sensitive high affinity binding of agonists to purified muscarinic receptors reconstituted with GTP-binding proteins (G_i and G_o). *J. Biol. Chem. 261*, 10133−10140.
(36) Peterson, G. L., Toumadje, A., Johnson, W. C., Jr., and Schimerlik, M. I. (1995) Purification of recombinant porcine m2 muscarinic acetylcholine receptor from Chinese hamster ovary cells. Circular dichroism spectra and ligand binding properties. *J. Biol. Chem. 270*, 17808−17814.
(37) Gomes, I., Jordan, B. A., Gupta, A., Rios, C., Trapaidze, N., and Devi, L. A. (2001) G protein coupled receptor dimerization: Implications in modulating receptor function. *J. Mol. Med. 79*, 226−242.
(38) Park, P. S., Filipek, S., Wells, J. W., and Palczewski, K. (2004) Oligomerization of G protein-coupled receptors: Past, present, and future. *Biochemistry 43*, 15643−15656.
(39) Zeng, F., and Wess, J. (2000) Molecular aspects of muscarinic receptor dimerization. *Neuropsychopharmacology 23*, S19−S31.
(40) Goin, J. C., and Nathanson, N. M. (2006) Quantitative analysis of muscarinic acetylcholine receptor homo- and heterodimerization in live cells: Regulation of receptor down-regulation by heterodimerization. *J. Biol. Chem. 281*, 5416−5425.
(41) Park, P. S., and Wells, J. W. (2004) Oligomeric potential of the M_2 muscarinic cholinergic receptor. *J. Neurochem. 90*, 537−548.
(42) Pisterzi, L. F., Jansma, D. B., Georgiou, J., Woodside, M. J., Chou, J. T., Angers, S., Raicu, V., and Wells, J. W. (2010) Oligomeric size of the M_2 muscarinic receptor in live cells as determined by quantitative fluorescence resonance energy transfer. *J. Biol. Chem. 285*, 16723−16738.
(43) Nakamura, S., and Rodbell, M. (1991) Glucagon induces disaggregation of polymer-like structures of the α subunit of the stimulatory G protein in liver membranes. *Proc. Natl. Acad. Sci. U.S.A. 88*, 7150−7154.
(44) Zhang, L., Yang, S., and Huang, Y. (2003) Evidence for disaggregation of oligomeric $G_o\alpha$ induced by guanosine-5′-3-O-(thio)triphosphate activation. *Biochemistry (Moscow) 68*, 121−128.
(45) Chidiac, P., and Wells, J. W. (1992) Effects of adenyl nucleotides and carbachol on cooperative interactions among G proteins. *Biochemistry 31*, 10908−10921.
(46) Tota, M. R., Kahler, K. R., and Schimerlik, M. I. (1987) Reconstitution of the purified porcine atrial muscarinic acetylcholine receptor with purified porcine atrial inhibitory guanine nucleotide binding protein. *Biochemistry 26*, 8175−8182.
(47) Ikegaya, T., Nishiyama, T., Haga, K., Haga, T., Ichiyama, A., Kobayashi, A., and Yamazaki, N. (1990) Interaction of atrial muscarinic receptors with three kinds of GTP-binding proteins. *J. Mol. Cell. Cardiol. 22*, 343−351.
(48) Sum, C. S., Park, P. S., and Wells, J. W. (2002) Effects of *N*-ethylmaleimide on conformational equilibria in purified cardiac muscarinic receptors. *J. Biol. Chem. 277*, 36188−36203.
(49) Chidiac, P., Green, M. A., Pawagi, A. B., and Wells, J. W. (1997) Cardiac muscarinic receptors. Cooperativity as the basis for multiple states of affinity. *Biochemistry 36*, 7361−7379.
(50) Ma, A. W.-S., Redka, D. S., Pisterzi, L. F., Angers, S., and Wells, J. W. (2007) Recovery of oligomers and cooperativity when monomers of the M_2 muscarinic cholinergic receptor are reconstituted into phospholipid vesicles. *Biochemistry 46*, 7907−7927.
(51) Park, P. S., and Wells, J. W. (2003) Monomers and oligomers of the M_2 muscarinic cholinergic receptor purified from *Sf*9 cells. *Biochemistry 42*, 12960−12971.
(52) Rasband, W. S. (1997−2012) *ImageJ*, National Institutes of Health, Bethesda, MD.
(53) Wells, J. W. (1992) in *Receptor-Ligand Interactions. A Practical Approach* (Hulme, E. C., Ed.) pp 289−395, Oxford University Press, Oxford, England.
(54) Redka, D. S., Pisterzi, L. F., and Wells, J. W. (2008) Binding of orthosteric ligands to the allosteric site of the M_2 muscarinic cholinergic receptor. *Mol. Pharmacol. 74*, 834−843.
(55) Aronstam, R. S., Hoss, W., and Abood, L. G. (1977) Conversion between configurational states of the muscarinic receptor in rat brain. *Eur. J. Pharmacol. 46*, 279−282.

(56) Ehlert, F. J., Roeske, W. R., and Yamamura, H. I. (1980) Regulation of muscarinic receptor binding by guanine nucleotides and *N*-ethylmaleimide. *J. Supramol. Struct. 14*, 149−162.
(57) Sum, C. S., Pyo, N., and Wells, J. W. (2001) Apparent capacity of cardiac muscarinic receptors for different radiolabeled antagonists. *Biochem. Pharmacol. 62*, 829−851.
(58) Sinkins, W. G., and Wells, J. W. (1993) G protein-linked receptors labeled by [^{3}H]histamine in guinea pig cerebral cortex. II. Mechanistic basis for multiple states of affinity. *Mol. Pharmacol. 43*, 583−594.
(59) Park, P. S., Sum, C. S., Pawagi, A. B., and Wells, J. W. (2002) Cooperativity and oligomeric status of cardiac muscarinic cholinergic receptors. *Biochemistry 41*, 5588−5604.
(60) Heitz, F., McClue, S. J., Harris, B. A., and Guenet, C. (1995) Expression of human M_2 muscarinic receptors in *Sf*9 cells: Characterisation and reconstitution with G-proteins. *J. Recept. Signal Transduction Res. 15*, 55−70.
(61) Knight, P. J., and Grigliatti, T. A. (2004) Diversity of G proteins in Lepidopteran cell lines: Partial sequences of six G protein α subunits. *Arch. Insect Biochem. Physiol. 57*, 142−150.
(62) Uustare, A., Nasman, J., Akerman, K. E., and Rinken, A. (2004) Characterization of M_2 muscarinic receptor activation of different G protein subtypes. *Neurochem. Int. 44*, 119−124.
(63) Zhang, Q., Okamura, M., Guo, Z. D., Niwa, S., and Haga, T. (2004) Effects of partial agonists and Mg^{2+} ions on the interaction of M_2 muscarinic acetylcholine receptor and G protein $G\alpha_{i1}$ subunit in the M_2-$G\alpha_{i1}$ fusion protein. *J. Biochem. 135*, 589−596.
(64) Seifert, R., Lee, T. W., Lam, V. T., and Kobilka, B. K. (1998) Reconstitution of β_2-adrenoceptor-GTP-binding-protein interaction in *Sf*9 cells. High coupling efficiency in a β_2-adrenoceptor-$G_{s\alpha}$ fusion protein. *Eur. J. Biochem. 255*, 369−382.
(65) Ehlert, F. J., and Rathbun, B. E. (1990) Signaling through the muscarinic receptor-adenylate cyclase system of the heart is buffered against GTP over a range of concentrations. *Mol. Pharmacol. 38*, 148−158.
(66) Hulme, E. C., Berrie, C. P., Birdsall, N. J., and Burgen, A. S. (1981) Two populations of binding sites for muscarinic antagonists in the rat heart. *Eur. J. Pharmacol. 73*, 137−142.
(67) Vanderheyden, P., Andre, C., de Backer, J. P., and Vauquelin, G. (1984) Agonist mediated conformational changes of solubilized calf forebrain muscarinic acetylcholine receptors. *Biochem. Pharmacol. 33*, 2981−2987.
(68) Bayburt, T. H., Vishnivetskiy, S. A., McLean, M. A., Morizumi, T., Huang, C. C., Tesmer, J. J., Ernst, O. P., Sligar, S. G., and Gurevich, V. V. (2011) Monomeric rhodopsin is sufficient for normal rhodopsin kinase (GRK1) phosphorylation and arrestin-1 binding. *J. Biol. Chem. 286*, 1420−1428.
(69) Haga, K., Kruse, A. C., Asada, H., Yurugi-Kobayashi, T., Shiroishi, M., Zhang, C., Weis, W. I., Okada, T., Kobilka, B. K., Haga, T., and Kobayashi, T. (2012) Structure of the human M_2 muscarinic acetylcholine receptor bound to an antagonist. *Nature 482*, 547−551.
(70) Vogel, W. K., Sheehan, D. M., and Schimerlik, M. I. (1997) Site-directed mutagenesis on the m2 muscarinic acetylcholine receptor: The significance of Tyr403 in the binding of agonists and functional coupling. *Mol. Pharmacol. 52*, 1087−1094.
(71) Gregory, K. J., Hall, N. E., Tobin, A. B., Sexton, P. M., and Christopoulos, A. (2010) Identification of orthosteric and allosteric site mutations in M_2 muscarinic acetylcholine receptors that contribute to ligand-selective signaling bias. *J. Biol. Chem. 285*, 7459−7474.
(72) Valant, C., Gregory, K. J., Hall, N. E., Scammells, P. J., Lew, M. J., Sexton, P. M., and Christopoulos, A. (2008) A novel mechanism of G protein-coupled receptor functional selectivity. Muscarinic partial agonist McN-A-343 as a bitopic orthosteric/allosteric ligand. *J. Biol. Chem. 283*, 29312−29321.
(73) Shivnaraine, R. V., Huang, X. P., Seidenberg, M., Ellis, J., and Wells, J. W. (2012) Heterotropic cooperativity within and between protomers of an oligomeric M_2 muscarinic receptor. *Biochemistry 51*, 4518−4540.
(74) Bock, A., Merten, N., Schrage, R., Dallanoce, C., Batz, J., Klockner, J., Schmitz, J., Matera, C., Simon, K., Kebig, A., Peters, L., Muller, A., Schrobang-Ley, J., Trankle, C., Hoffmann, C., De Amici, M., Holzgrabe, U., Kostenis, E., and Mohr, K. (2012) The allosteric vestibule of a seven transmembrane helical receptor controls G-protein coupling. *Nat. Commun. 3*, 1044.
(75) Vivo, M., Lin, H., and Strange, P. G. (2006) Investigation of cooperativity in the binding of ligands to the D_2 dopamine receptor. *Mol. Pharmacol. 69*, 226−235.
(76) Casado, V., Ferrada, C., Bonaventura, J., Gracia, E., Mallol, J., Canela, E. I., Lluis, C., Cortes, A., and Franco, R. (2009) Useful pharmacological parameters for G-protein-coupled receptor homodimers obtained from competition experiments. Agonist-antagonist binding modulation. *Biochem. Pharmacol. 78*, 1456−1463.
(77) Urizar, E., Montanelli, L., Loy, T., Bonomi, M., Swillens, S., Gales, C., Bouvier, M., Smits, G., Vassart, G., and Costagliola, S. (2005) Glycoprotein hormone receptors: Link between receptor homodimerization and negative cooperativity. *EMBO J. 24*, 1954−1964.
(78) Albizu, L., Balestre, M. N., Breton, C., Pin, J. P., Manning, M., Mouillac, B., Barberis, C., and Durroux, T. (2006) Probing the existence of G protein-coupled receptor dimers by positive and negative ligand-dependent cooperative binding. *Mol. Pharmacol. 70*, 1783−1791.
(79) Kara, E., Lin, H., and Strange, P. G. (2010) Co-operativity in agonist binding at the D_2 dopamine receptor: Evidence from agonist dissociation kinetics. *J. Neurochem. 112*, 1442−1453.
(80) Albizu, L., Cottet, M., Kralikova, M., Stoev, S., Seyer, R., Brabet, I., Roux, T., Bazin, H., Bourrier, E., Lamarque, L., Breton, C., Rives, M. L., Newman, A., Javitch, J., Trinquet, E., Manning, M., Pin, J. P., Mouillac, B., and Durroux, T. (2010) Time-resolved FRET between GPCR ligands reveals oligomers in native tissues. *Nat. Chem. Biol. 6*, 587−594.
(81) Neri, M., Vanni, S., Tavernelli, I., and Rothlisberger, U. (2010) Role of aggregation in rhodopsin signal transduction. *Biochemistry 49*, 4827−4832.
(82) Pin, J. P., Kniazeff, J., Liu, J., Binet, V., Goudet, C., Rondard, P., and Prezeau, L. (2005) Allosteric functioning of dimeric class C G-protein-coupled receptors. *FEBS J. 272*, 2947−2955.
(83) Han, Y., Moreira, I. S., Urizar, E., Weinstein, H., and Javitch, J. A. (2009) Allosteric communication between protomers of dopamine class A GPCR dimers modulates activation. *Nat. Chem. Biol. 5*, 688−695.
(84) Baneres, J. L., and Parello, J. (2003) Structure-based analysis of GPCR function: Evidence for a novel pentameric assembly between the dimeric leukotriene B_4 receptor BLT1 and the G-protein. *J. Mol. Biol. 329*, 815−829.
(85) Filipek, S., Krzysko, K. A., Fotiadis, D., Liang, Y., Saperstein, D. A., Engel, A., and Palczewski, K. (2004) A concept for G protein activation by G protein-coupled receptor dimers: The transducin/rhodopsin interface. *Photochem. Photobiol. Sci. 3*, 628−638.
(86) Vidi, P. A., Chen, J., Irudayaraj, J. M., and Watts, V. J. (2008) Adenosine A_{2A} receptors assemble into higher-order oligomers at the plasma membrane. *FEBS Lett. 582*, 3985−3990.
(87) Carriba, P., Navarro, G., Ciruela, F., Ferre, S., Casado, V., Agnati, L., Cortes, A., Mallol, J., Fuxe, K., Canela, E. I., Lluis, C., and Franco, R. (2008) Detection of heteromerization of more than two proteins by sequential BRET-FRET. *Nat. Methods 5*, 727−733.
(88) Guo, W., Urizar, E., Kralikova, M., Mobarec, J. C., Shi, L., Filizola, M., and Javitch, J. A. (2008) Dopamine D2 receptors form higher order oligomers at physiological expression levels. *EMBO J. 27*, 2293−2304.
(89) Hern, J. A., Baig, A. H., Mashanov, G. I., Birdsall, B., Corrie, J. E., Lazareno, S., Molloy, J. E., and Birdsall, N. J. (2010) Formation and dissociation of M_1 muscarinic receptor dimers seen by total internal reflection fluorescence imaging of single molecules. *Proc. Natl. Acad. Sci. U.S.A. 107*, 2693−2698.
(90) Calebiro, D., Rieken, F., Wagner, J., Sungkaworn, T., Zabel, U., Borzi, A., Cocucci, E., Zurn, A., and Lohse, M. J. (2013) Single-molecule analysis of fluorescently labeled G-protein-coupled receptors reveals complexes with distinct dynamics and organization. *Proc. Natl. Acad. Sci. U.S.A. 110*, 743−748.
(91) Golebiewska, U., Johnston, J. M., Devi, L., Filizola, M., and Scarlata, S. (2011) Differential response to morphine of the oligomeric state of μ-opioid in the presence of δ-opioid receptors. *Biochemistry 50*, 2829.

(92) Herrick-Davis, K., Grinde, E., Lindsley, T., Cowan, A., and Mazurkiewicz, J. E. (2012) Oligomer size of the serotonin 5-hydroxytryptamine 2C (5-HT_{2C}) receptor revealed by fluorescence correlation spectroscopy with photon counting histogram analysis: Evidence for homodimers without monomers or tetramers. *J. Biol. Chem. 287*, 23604−23614.
(93) Ianoul, A., Grant, D. D., Rouleau, Y., Bani-Yaghoub, M., Johnston, L. J., and Pezacki, J. P. (2005) Imaging nanometer domains of β-adrenergic receptor complexes on the surface of cardiac myocytes. *Nat. Chem. Biol. 1*, 196−202.
(94) Milligan, G. (2010) The role of dimerisation in the cellular trafficking of G-protein-coupled receptors. *Curr. Opin. Pharmacol. 10*, 23−29.
(95) Milligan, G. (2009) G protein-coupled receptor hetero-dimerization: Contribution to pharmacology and function. *Br. J. Pharmacol. 158*, 5−14.
(96) Bayburt, T. H., Leitz, A. J., Xie, G., Oprian, D. D., and Sligar, S. G. (2007) Transducin activation by nanoscale lipid bilayers containing one and two rhodopsins. *J. Biol. Chem. 282*, 14875−14881.
(97) Ernst, O. P., Gramse, V., Kolbe, M., Hofmann, K. P., and Heck, M. (2007) Monomeric G protein-coupled receptor rhodopsin in solution activates its G protein transducin at the diffusion limit. *Proc. Natl. Acad. Sci. U.S.A. 104*, 10859−10864.
(98) Whorton, M. R., Bokoch, M. P., Rasmussen, S. G., Huang, B., Zare, R. N., Kobilka, B., and Sunahara, R. K. (2007) A monomeric G protein-coupled receptor isolated in a high-density lipoprotein particle efficiently activates its G protein. *Proc. Natl. Acad. Sci. U.S.A. 104*, 7682−7687.
(99) Wong, H. M., Sole, M. J., and Wells, J. W. (1986) Assessment of mechanistic proposals for the binding of agonists to cardiac muscarinic receptors. *Biochemistry 25*, 6995−7008.